Transcriptional and Progesterone Receptor Binding Profiles of the Human Endometrium Reveal Important Pathways and Regulators in the Epithelium During the Window of Implantation

Ru-pin Alicia Chi[1], Tianyuan Wang[2], Nyssa Adams[3], San-pin Wu[1], Steven L. Young[4], Thomas E. Spencer[5,6], and Francesco DeMayo[1]

[1] Reproductive and Developmental Biology Laboratory, National Institute of Environmental Health Sciences, Research Triangle Park, North Carolina, USA

[2] Integrative Bioinformatics Support Group, National Institute of Environmental Health Sciences, Research Triangle Park, North Carolina, USA

[3] Interdepartmental Program in Translational Biology and Molecular Medicine, Baylor College of Medicine, Houston, Texas, USA

[4] Department of Obstetrics and Gynecology, University of North Carolina at Chapel Hill, Chapel Hill, North Carolina, USA

[5] Division of Animal Sciences and [6]Department of Obstetrics, Gynecology and Women's Health, University of Missouri, Columbia, Missouri, USA

ABSTRACT

The endometrium undergoes highly dynamic modifications in a time and compartment specific manner during each menstrual cycle resulting in full receptivity to embryo implantation during a discrete temporal window of implantation (WOI). Attainment of normal receptivity is strictly governed by the steroid hormone progesterone, which acts via the two isoforms of the nuclear Progesterone Receptor (PGR). In order to define the molecular mechanisms regulated by PGR in uterine receptivity, we conducted RNA-sequencing and PGR ChIP-sequencing (ChIP-seq) in endometrial biopsies taken from fertile women during the proliferative (P) and mid-secretory (MS) phases. Overlaying the genes with altered PGR binding and differential expression (DEGs) during the phase transition identified 653 genes, which are involved in inflammatory response signaling, xenobiotic metabolism, epithelial-mesenchymal transition (EMT), cell death regulation, interleukin/STAT signaling, estrogen response, as well as MTORC1 response. RNA-sequencing conducted using epithelium-derived RNA identified 3,052 DEGs in the epithelium, of which 658 were uniquely regulated in the epithelium. Transcription factors IRF8 and MEF2C were selected for validation and found to be regulated in the epithelium during the WOI at the protein level, suggesting potentially important functions that are previously unrecognized. In summary, we present herein data that expands our understanding of the progesterone action in human endometrium during the WOI.

Introduction

The human endometrium is a highly complex tissue. The functionalis layer consists of the stromal compartment which makes up significant portion of the endometrium; the glandular epithelium which is responsible for secreting an array of growth factors and cytokines [1]; and the luminal epithelium which lines the stromal compartment and is the first maternal cell type with which the embryo interacts inside the uterus. In order to maximize the chances of a successful pregnancy, the uterus prepares for embryo implantation after each menstruation by the generation and differentiation of the endometrial functionalis, a process known as the menstrual cycle [2, 3]. This is orchestrated by the interplay of two steroid hormones, estrogen and progesterone. During the proliferative (P) phase, estrogen promotes proliferation of both the stromal and epithelial cells, steadily increasing the thickness of the functionalis [4, 5]. Upon ovulation, the ovary begins secreting significant amounts of progesterone, halting estrogen-induced proliferation and initiating a dramatic pattern of differentiation of stromal cells (decidualization) and epithelial cells. These include depolarization, altered surface morphology, expression of specific adhesion proteins, altered steroid receptor expression, and secretion of glycogen [5, 6]. Without a successful implantation, the levels of both steroid hormones decrease during the late secretory phase, leading to endometrial involution and subsequently endometrial shedding (menstruation), initiating another cycle [7].

Abnormal embryo implantation and implantation failure is a major cause of infertility and early pregnancy loss and is linked to other pregnancy complications [8-12]. Attainment of human endometrial receptivity occurs in the mid-secretory phase (MS) after sufficient time and concentration of progesterone exposure as seen in other placental mammals [13-18]. In women

without ovaries, sequential treatment with estrogen followed by estrogen plus progesterone, without any other ovarian hormones, is sufficient to achieve high rates of successful implantation of embryos derived from donor oocytes [16, 19], though successful pregnancy establishment largely depends on length of progesterone exposure [20].

Abnormal progesterone signaling leads not only to fertility issues but also a spectrum of gynecological diseases [21-23], emphasizing the criticality of progesterone signaling in maintaining normal uterine biology and initiating pregnancy. The impact of progesterone is mediated through its nuclear receptor – the progesterone receptor (PGR), where binding of progesterone induces a conformational change of the receptor, leading to affinity change for target DNA response elements and thereby influencing the gene expression network at the transcriptional level [24]. The PGR itself exhibits the highest expression level during the late P phase, followed by a gradual decrease reaching the lowest expression in the late secretory phase [25]. To date, many PGR-regulated genes have been identified in both animal model systems and human studies as important mediators of implantation, including Indian Hedgehog (*IHH*) [26-28], Krüpple-like Factor 15 (*KLF15*) [29, 30], Heart and Neural Crest Derivatives-expressed 2 (*HAND2*) [31], Bone Morphogenesis Protein 2 (*BMP2*) [32, 33], Homeobox gene *HOXA10* [30, 34, 35], CCAAT/Enhancer-binding Protein β (*CEBPB*) [36-38], and many others [14]. Yet, implantation failure remains a great challenge in both natural pregnancies and assisted reproductive interventions.

Epithelial aspects of PGR actions are important, sometimes underappreciated determinants of implantation and pregnancy outcome. Endometrial epithelial cells line the uterine lumen and glands, with the latter derived from the former [39, 40]. The endometrial epithelium undergoes

dramatic cellular and molecular changes common to both mouse models and humans during the WOI, including adhesion mechanisms enabling the attachment of embryo to the luminal epithelium [41, 42], alterations in nuclear pore complex presentation [43], downregulation of the Serum and Glucocorticoid Regulated Kinase 1 (SGK1) [44], apoptotic cascade [45, 46], and expression of epithelial-specific receptivity markers [47]. The glandular epithelium which is regulated by FOXA2 signaling further facilitates implantation via the production of Leukemia Inhibitory Factor (LIF), which is a critical factor in embryo-uterine communication leading to successful implantation [48-50]. Elaborate cross-talk also exists between the endometrial epithelium and stroma that is indispensable for allowing implantation, adding further complexity to the regulatory mechanisms governing pregnancy establishment. For example, epithelial-stromal cross-talk has been well documented for the IHH pathway, where epithelial derived IHH regulates stromal functions through COUP-TFII and HAND2 prior to implantation in a mouse model [26-28]. These findings further highlight the intricacy of the endometrial mechanisms allowing normal implantation, highlighting the need for understanding the contributions of each cell type and the interactions between them.

The decades long efforts devoted to understanding implantation using animal model systems or *in vitro* cultured cells have yielded fruitful outcomes and proven instrumental in advancing our current knowledge in reproductive functions. The high rate of embryonic losses due to implantation failure, however, remain a challenge [51]. The aim of this study is to use a single, comparative, human-derived, *ex vivo* analysis to examine the dynamics of PGR action during the WOI. We employed ChIP-seq technique to explore the modification of PGR binding landscape during the P to MS transition in human endometrial samples. Additionally, parallel RNA-sequencing analysis enabled the identification of PGR binding genes, enabling us to identify the subset of PGR-bound genes which displayed altered mRNA abundance and hence relevance in

regulating implantation and decidualization. Epithelial-specific RNA-sequencing allowed more precise assessment of the endometrial epithelial transcriptomic network allowing a deeper knowledge of the dynamic transformation in the endometrium during the WOI.

Results

Characterization of PGR binding trend during the P and MS phases

To gain insights into the transcriptional regulatory function of PGR during the peri-implantation period, the physical association of PGR with DNA was assessed by PGR chromatin immunoprecipitation coupled to massively parallel DNA sequencing (ChIP-seq) using human endometrial biopsies from the P and MS phases. In total, 11,893 and 16,283 genomic intervals were identified as PGR bound in the P and MS endometrium, respectively, and 9,367 intervals were occupied by PGR in both phases. Analysis using the Peak Annotation and Visualization tool showed that majority of the PGR binding occurred within the intronic, intergenic, 5' UTR and upstream region relative to the gene body, with no significant alteration in PGR binding preference to these categories between the two phases (Fig. 1. A).

The alteration in PGR binding trend between the two phases was examined. Collectively, we analyzed two sets of samples, each containing a P and MS pair. To circumvent the batch variation observed between the two sets, we only considered differential PGR binding (DPRB) between the phases of the menstrual cycle that were identified as common between the two independent sets (Fig. 1. B). A total of 13,371 DPRB intervals were identified during the P to MS transition in the endometrium. After adjusting for basal peak values, 7,272 DPBR intervals were determined as intervals with "real" PGR binding (in at least one of the two stages), of which 2,787 were located within 25 kb of the transcriptional start site (TSS ± 25 kb) of 2,249 unique genes (Fig. 1. B, Supplemental Material 1). There were 2,466 intervals with increased PGR binding in proximity to 1,966 genes (88%) and 321 intervals with decreased PGR binding in proximity to 307 genes

(12%, Fig. 1. C), and 423 genes were found with multiple differential PGR binding intervals in proximity.

Amongst the identified DPRB intervals, many were found in proximity to known PGR-regulated genes previously reported in both humans and mice, including FK506 Binding Protein 5 (*FKBP5*) [30], Indian Hedgehog (*IHH*), Insulin Receptor Substrate 2 (*IRS2*) [52], *CASP8* and FADD Like Apoptosis Regulator (*CFLAR*) [53], FOS Like 2 AP-1 Transcription Factor Subunit (*FOSL2*) [30], Perilipin 2 (*PLIN2*), Basic Leucine Zipper ATF-Like Transcription Factor (*BATF*) and Baculoviral IAP Repeat Containing 5 (*BIRC5*) [22]. In addition, many known decidualizing and implantation mediators were found with proximal PGR binding, although binding was not necessarily shown to be differential between the cycle phases, including Forkhead Box Protein O1 (*FOXO1*) [54], Homeobox A10 (*HOXA10*) [54], Interferon Regulatory Factor 4 (*IRF4*) [55], Heart And Neural Crest Derivatives Expressed 2 (*HAND2*) [2], Cysteine Rich Angiogenic Inducer 61 (*CYR61*) [30] and Sex Determining Region Y-Box 17 (*SOX17*) [56, 57]. The biological impact of PGR transcriptional activity during the P to MS phase was determined by examining the functional profile associated with the DPRB genes using the DAVID bioinformatics tool [58, 59], and selected enriched pathways are shown in Table 1. Enrichment was observed in pathways regulating insulin resistance, focal adhesion, complement and coagulation cascades, cytokine-cytokine receptor interactions, ECM receptor interaction, apoptosis, as well as various signaling pathways including chemokines, Ras, FOXO, Prolactin, AMPK and Tumor Necrosis Factor (TNF). In addition, Gene Ontology functional annotation showed that the DPRB-associated genes are involved in the regulation of cell migration, signal transduction, angiogenesis, vasculature development and secretion (Fig. 1. D).

Despite the decrease in PGR expression during the MS phase (Supplemental Material 2, see below), the global PGR binding trend was elevated as 88% of the intervals differentially bound by PGR exhibited increased binding during the MS phase (Fig. 1. C), and this is likely due to the increased level of progesterone in this phase of the cycle. To further explore enrichment of other transcription factor binding sites co-occupying the PGR binding intervals, the DPRB DNA motifs were analyzed by HOMER in two parts; those that showed elevated binding during MS (MS-gain) or reduced binding during MS (MS-loss). The MS-gain intervals, indeed, showed significant enrichment in PGR binding motif with a *p*-value of 1.00^{-40} (Table 2). MS-gain and MS-loss intervals exhibited distinct profiles of additional transcription factor binding site preferences, with *FOSL2*, *FRA1*, *JUN-AP1*, *ATF3* and *BATF* binding domains as top enriched binding sites in MS-gain intervals (Table 2). Nuclear Receptors *AR*, bZIP transcription factor *CHOP* and some STAT transcription factor members *STAT1*, *STAT3* and *STAT5* binding sites were also enriched in sites with increased PGR binding (Table 2). In contrast, enriched motifs in the MS-loss intervals included Estrogen Response Element (ERE), and binding domains for Transcription Factor 21 (*TCF21*), Atonal BHLH Transcription Factor 1 (*ATOH1*), Zinc Finger And BTB Domain Containing 18 (*ZBTB18*), as well as GLI Family Zinc Finger 3 (*GLI3*, Table 3). Of note, during the P to MS transition, PGR showed an increased preference for the Basic Leucine Zipper Domain (bZIP), as the MS-gain intervals belonged mainly to this class. On the other hand, preference for the Basic Helix Loop Helix (bHLH) and Zinc Finger (ZF) binding domains were lost during this phase transition, as the enriched motifs identified in the MS-loss intervals belonged mainly to these two groups. Thus, PGR's effects on gene expression may be partially modulated through altered affinity for the different DNA responsive elements between the liganded and unliganded form.

Transcriptional regulatory network of the P and MS endometrium

Whilst PGR has been widely studied in both humans and rodents and many direct and indirect target genes have been identified, a comprehensive analysis revealing its global regulatory function in the cycling human endometrium is still lacking. To fully characterize the functional relevance associated with PGR binding activities during the P to MS transition, we conducted RNA-seq on whole endometrium and incorporated the global gene expression profile into the ChIP-seq analyses during these two phases.

In total, we collected six P and five MS endometrial biopsies from which whole endometrial RNA was analyzed. This revealed a total of 14,985 expressed genes within the whole endometrium (FPKM > 1 in at least one of the two phases), whereby 14,303 and 14,156 were expressed in each of the P and MS phase, respectively. The transcriptomic profiles were subjected to hierarchical clustering and principal component analysis (PCA) as a measure of quality control. As shown in Figure 2. A, a distinct segregation was observed for the P- and MS-derived RNA expression profile, and this is further supported by the hierarchical clustering presented in the dendrogram shown in Fig. 2. B, where samples from the two stages clustered accordingly. This suggested that the samples were well-characterized according to stage and of appropriate quality.

Of the genes expressed in the endometrium, 4,576 were differentially expressed (DEGs, Supplemental Material 2) between the two phases (absolute fold change > 1.5; and adjusted *p* value < 0.05). In total, 2,392 genes showed increased expression while 2,184 were downregulated during MS. Several genes known to regulate uterine biology, decidualization and implantation were identified as DEGs including: decidualizing markers IGF Binding Protein 1 (*IGFBP1*) and prolactin (*PRL*); hedgehog protein, Indian Hedgehog (*IHH*); transcription factors

FOXO1 and *GATA2*; Wnt signaling molecules *WNT4*, *WNT2*, *WNT5A* and their inhibitor *DKK1*; transcriptional repressor *ZEB1*; and extracellular matrix modulator *VCAN*. To interpret the biological impact of the DEGs during the P to MS transition, Gene Set Enrichment Analysis (GSEA) was performed to retrieve the functional profile associated with the DEGs [60]. Consistent with current literature, elevated inflammatory response was identified as an enriched molecular function for the DEGs associated with the P to MS transition, as indicated by the positive enrichment in the TNFA-NFKB signaling axis, coagulation, allograft rejection, hypoxia, the complement cascade, interferon gamma response, IL6-JAK-STAT3 signaling and apoptosis (Table 4). On the other hand, the negatively enriched functions which represents repressed molecular pathways during MS showed significance in cell division regulatory mechanisms – including E2F targets, G2M checkpoint and mitotic spindle regulations (Table 4). The xenobiotic metabolism pathway was identified as one of the most positively enriched functions in the MS endometrium by both GSEA (Table 4, Fig. 2. C) and Ingenuity Pathway Analysis (data not shown). To validate the RNA-seq results, we examined expression of selected xenobiotic metabolism genes using RNA extracted from another set of endometrial biopsies (n = 6 for each of the P and MS phase), along with the expression of the decidualization markers *PRL* and *IGFBP1* to confirm the sample stages (Figs. 2. D and E). In accordance with the RNA-seq results (Fig. 2. F), the cytochrome P450 members *CYP2C18* and *CYP3A5*, solute carriers *SLC6A12* and *SLCO4A1*, and glucuronosyltransferase *UGT1A6* were all found to be upregulated during MS (Fig. 2. G). Further, glutathione S-transferase Mu genes (*GSTM1*, *GSTM3* and *GSTM5*), sulfotransferase *SULT1C4*, and solute carrier *SLCO2A1* were found to be repressed during the MS phase (Fig. 2. I) similarly to that observed with RNA-seq (Fig. 2. H).

Functional profiling of DEGs with regulated PGR binding during P to MS

To search for the genes that are potentially directly regulated by PGR and important in modulating implantation, we identified the genes that were both differentially expressed and differentially bound by PGR in the whole endometrium between the P and MS phases. Comparison of DEGs and DPRB gene lists revealed 653 genes common to both datasets (Fig. 3. A). The trend for PGR binding and altered gene expression during MS, as compared to P is summarized in Table 5 and graphically presented in Figure 3. B. This analysis found 87% of the genes showed increased PGR binding (572 out of 653), and 70% showed upregulation during the MS phase (454 out of 653). Interestingly, the majority of these genes showed a positive correlation between PGR binding change and transcriptional regulation, i.e. increased PGR binding was associated with increased gene expression and vice versa. Thus, PGR binding generally promotes rather than represses gene expression in the human endometrium (Fig. 3. C).

The physiological function of PGR in regulating endometrial biology was next examined by elucidating the enriched functions associated with the PGR-regulated DEGs during the P to MS shift. The genes, along with fold change were submitted to GSEA to examine the enrichment of biological functions (Table 6). Enrichment was observed for a wide range of biological processes including inflammatory response signaling (coagulation, TNFA signaling via NFKB, complement, hypoxia, interferon gamma response), xenobiotic metabolism, epithelial mesenchymal transition (EMT), cell death regulation (apoptosis, p53 pathway), interleukin/STAT signaling, estrogen response, and MTORC1 response. Many of these biological functions were similarly identified using the DAVID Bioinformatic Database such as the regulation of cell death, inflammatory response, cytokine production, response to hormone and response to oxygen levels (Supplemental Material 3). Additionally, “secretion by cell” was identified as a regulated pathway by DAVID (p = 6.60E-5), confirming the validity of the secretory-phase derived gene expression

profile. Other pathways identified by DAVID included cell migration, signal transduction, angiogenesis, leucocyte migration, nitric oxide biosynthetic processes, ECM disassembly, and various activities associated with lipid regulation and insulin response (Supplemental Material 3).

To authenticate the ChIP-seq results and the regulatory role of PGR, PGR-chromatin association was evaluated for selected genes from the apoptosis and EMT pathways, both of which are known to regulate receptivity. In addition, we examined PGR binding near the MAF bZIP Transcription Factor (*MAF*), a regulator of the xenobiotic metabolism pathway shown earlier to be positively enriched during MS. Two known PGR-regulated genes in the human endometrial cells, *IHH* and *FOSL2* were first validated and confirmed to show increased (*FOSL2*) and decreased (*IHH*) PGR binding during the MS phase (Figs. 3. D and 3. E). Apoptosis regulating genes Epithelial Membrane Protein 1 (*EMP1*), Immediate Early Response 3 (*IER3*), and B-Cell CLL/Lymphoma 2 Like 10 (*BCL2L10*), as well as EMT mediators GTP Binding Protein Overexpressed In Skeletal Muscles (*GEM*) and Serpin Family E Member 1 (*SERPINE1*), all displayed elevated PGR binding during the MS phase indicated by independent ChIP-qPCR analysis (Fig. 3. F). Additionally, independent qPCR analysis revealed the elevated transcription of apoptotic modulators (*EMP1*, *IER3* and *BCL2L10*) and the EMT regulator *SERPINE1*. Other genes regulating these two pathways were also found to be transcriptionally regulated, including Glutathione Peroxidase 3 (*GPX3*), Tissue Inhibitor Of Metalloproteinases 3 (*TIMP3*), Vanin 1 (*VNN1*), Nicotinamide N-Methyltransferase (*NNMT*) and Transglutaminase 2 (*TGM2*, Fig. 3. G).

To identify potential regulators controlled by or associated with PGR, we next used IPA to predict for activity of upstream regulators based on the 653 common genes (DEG + DPRB), and DEGs without differential PR binding (DEG – DPRB, 3,923 genes) were used for comparison. (Fig. 3.

A, the “purple” genes and the “blue” genes, respectively). Comparison of the upstream regulator activity showed a higher Z-score for both progesterone and FOXO1 (a known co-factor of PGR) in the regulation of the DEG + DPRB genes compared to the DEG – DPRB genes (Fig. 3. H), confirming that this group of genes is more closely associated with with the progesterone-PGR signaling. Amongst the upstream regulators predicted for each gene set, the inflammation associated transcription factor NFKB family including REL, RELB and NFKB2 all possessed a stronger activation score in the DEGs + DPRB (Fig. 4. H), suggesting enhanced activity based on the altered gene expression network. In addition to NFKB, the angiogenic modulators ANGPT2 and VEGF, developmental regulators HOXD10 and SOX4, histone modifier KAT5 and the kinase MAP2K4 were all regulators predicted to have a higher activation score in regulating the group of genes with differential PGR binding. Interestingly, the cell cycle regulator CCND1, transcriptional regulators FOXM1 and MITF, prostaglandin receptor PTGER2 and the kinase protein ERBB2 were all predicted to be strongly inhibited in the regulation of DEG - DPRB, but Z-score prediction suggest that those factors were not inhibited in the regulation of the DEGs + DPRB. This suggests although PGR may not directly inhibit these factors they may engage with PGR in a co-operative manner to regulate the downstream gene expression network. Moreover, the MET-HGF receptor ligand pair as well as fat metabolism modulators PLIN5, LEPR and Insulin I were all found with increased activity in regulating the DEGs + DPRB, suggesting that these signaling axes are also associated with PGR function in the cycling human uterus. Interestingly, although Insulin (*INS*) itself was not transcriptionally regulated during the P to MS cycle, its cognate receptor Insulin Receptor (*INSR*) showed strong transcriptional induction (Supplemental Material 2). Additionally, many genes known to be regulated by insulin including *TIMP3* (Fig. 3. G, Supplemental Material 2), *SOD2*, *SOCS3*, *PRLR* and *MMP2* all showed elevated mRNA expression in the MS endometrium (Supplemental Material 2).

Epithelial transcriptome in the cycling endometrium

To further understand the complexity of the cycling uterus, we assessed transcriptional changes in the epithelial lining of the endometrium. As the endometrium consists of a complex and dynamically changing set of cells, gene expression profiles derived from whole endometrial biopsies often overlook alterations of specific cell types. Four P and five MS endometrial samples were obtained, from which the epithelial RNA was extracted and subjected to RNA-seq analysis. Principal component analysis (PCA) and hierarchical clustering found good segregation of the gene expression profile derived from two differently staged samples (Fig. 4. A and B). In the epithelium, we found a comparable number of genes expressed to that of the whole endometrium, with 14,502 genes and 13,993 genes transcriptionally active during the P and MS phase, respectively. The same threshold for identifying DEGs in the whole endometrium was applied to the epithelium-expressed genes, with which 3,052 epithelial-specific DEGs were found (epi-DEGs, Supplemental Material 4). Of those, 57% (1,764) showed elevated transcription and 43% (1,288) was transcriptionally repressed during the MS phase. Functional enrichment analysis of the epi-DEGs using GSEA showed a positive enrichment for the genes encoding components of the apical junction complex (Table 7), a molecular process important in defining the polarity of the epithelium and hence supports the authenticity of the gene expression profile obtained from an epithelial origin. Most of the pathways identified for the epithelium, whether positively or negatively enriched, were principally similar to that of the whole endometrium, with enrichment in pathways regulating immune responses including coagulation, complement, TNFA signaling via NFKB, apoptosis, as well as xenobiotic metabolism. On the other hand, cell division related processes including E2F regulated cell cycle, G2M checkpoint, mitotic spindle and DNA repair were negatively enriched (Table 7).

Functions specific to the endometrial epithelium during implantation

To tease out the epithelial specific molecular events, we next compared the whole endometrium DEG with the epi-DEG to identify DEGs that are unique to the epithelium. In total, 2,411 common genes were found, representing those that show differential expression in both the whole endometrium and epithelium (Fig 4. C, Supplemental Materials 2 and 4). Of those, 2,394 genes showed the same transcriptional change between the two compartments, and 17 genes, although identified as “common” DEGs, exhibited the reversed change in mRNA level between the two compartments. Altogether with the 641 genes which were exclusively regulated in the epithelium, a total of 658 genes which were “specifically” regulated in the epithelium was found. Canonical pathways regulated by this group of genes were assessed using IPA and ranked according to significance in Table 8. Synthesis of glycosaminoglycans, including dermatan sulfate and chondroitin sulfate, as well as cholesterol biosynthesis were the most significant pathways identified (-Log *p* value > 3). Osteoarthritis pathway, cholecystokinin/gastrin mediated signaling, IL8 signaling and TGFB signaling were all significant pathways with a positive Z-score, suggesting increased activity during MS in the endometrial epithelium. On the other hand, PTEN signaling was identified as significantly repressed in the MS epithelium (Table 8).

IPA was next used to predict for upstream regulator activities in the epithelium (Supplemental Material 5). As expected, both progesterone and PGR were identified as activated upstream regulators, with Z-score values of 2.269 and 3.812, and *p* values of 1.77E-46 and 1.29E-29, for progesterone and PGR, respectively. Estrogen Receptor Alpha (ESR1) was shown to be repressed while ESR2 was activated. Interestingly, RNA-seq results illustrated decreased expression of *ESR1* and upregulation of *ESR2* in the MS epithelium. The top activated regulators were cytokines including IL1B, TNF, IFNG, OSM and IL1A; as well as transcriptional regulators such as NUPR1, NFKB, TBX2, SMARCA4 and CEBPA (Z-score > 5). Repressed regulators

included transcription factors TBX2, TAL1; small GTPase RABL6, catenin protein CTNNA1, as well as the E1A Binding Protein P400 (EP400).

Lastly, to identify regulators with specific activities in the epithelium during the MS phase, we cross-compared the upstream regulators identified for the whole endometrium DEGs and epithelial DEGs. To ensure that the upstream regulators identified were meaningful and relevant, we compared only the regulators with *p*-values less than 0.05, and the numerical activation Z-score values greater than 1.5. This comparison yielded several regulator proteins with specific actions in the epithelium, of which selected are shown in Table 9. Amongst those were transcriptional regulators POU5F1, IRF5, IRF8 and FOXJ1; Myocyte Enhancer Factors family MEF2C and MEF2D; transmembrane receptors TLR5, IL1R1 and FCGR2A; kinase proteins MET and AURKB; the growth factor HBEGF; the CYP27B1 enzyme and Wnt ligand WNT7A; as well as the Notch ligand DLL4. Interestingly, *MEF2C*, *MEF2D*, *IRF8*, *FOXJ1*, *HBEGF*, *CYP27B1* and *DLL4* were found to be uniquely regulated in the epithelium, where either transcriptional regulation was not detected in the whole endometrium or showed a different pattern of gene expression during the P to MS transition. In addition, *HBEGF* was expressed at very low levels as indicated by an average FPKM value of 2.63 in the whole endometrium; compared to 19.26 in the epithelium (data not shown), suggesting that the transcription of this gene is enriched in the epithelial cells during the WOI. We examined the protein expression of two epithelial-specific regulators IRF8 and MEF2C using formalin-fixed and paraffin-embedded endometrial biopsies from independent patients. As shown in Figure 5. A, IRF8 is expressed in both stromal and epithelial cells but exhibited elevated protein expression specifically in the glandular epithelium during the MS phase. MEF2C, on the other hand, displayed a robust cytoplasmic-to-nuclear translocation from the P to MS stage specifically in the glandular epithelium. These results suggest that both IRF8 and MEF2C, two proteins previously unreported to have a role in implantation are regulated both at

the mRNA and protein level during the peri-implantation phase of the menstrual cycle in the epithelium, and hence may have important functions in the implantation-phase endometrium.

Discussion

Here, we investigated the cycling human endometrium at the molecular level with two major aims in mind. First, to gain better understanding of the human endometrial signaling pathways and molecular events controlled by PGR during the P to MS transition. Combining the PGR cistromic and whole endometrium transcriptomic profile allowed the identification of genes with both proximal PGR binding and transcriptional regulation during the WOI. Second, we examined the gene expression profile using RNA derived from the whole endometrium or from the epithelium. Comparison of the two expression profiles delineated a more sophisticated and compartment specific transcriptional network. The latter has remained a challenging task and for this reason, the endometrium has often been examined as a whole when conducting *in vivo* studies.

The biological significance of PGR transcriptional activity during the WOI

Using PGR ChIP-seq, we obtained a genome wide DNA-binding blueprint of PGR in the endometrium at the P and MS phases. Comparison of the two enabled the identification of DEGs with regulated PGR binding in proximity during this period. Using the motif finding tool HOMER, we found a distinguishing difference in PGR binding preference from P to MS. While sites with increased PGR bindings at MS were predominantly co-occupied by bZIP and STAT transcription factors, sites with reduced PGR binding during MS were shared by bHLH and ZF transcription factors. This finding may suggest a mechanism of regulation for PGR transcriptional activity whereby its preference for certain DNA motifs are gained or lost during different phases of the menstrual cycle. Alternatively, the association of PGR to these DNA motifs may not be a direct one, but rather through interaction with other transcription factors which then associate with the promoter region. The changes in DNA motifs detected based on altered PGR binding could in

turn suggest a change in PGR preference for different transcription factors rather than different DNA motifs. Indeed, PGR is known to control gene expression in this way through transcription factors such as SP1 and AP1 in human endometrial cells and mammary cells [30, 61, 62].

A more comprehensive landscape of PGR biological impact was achieved by comparing the whole endometrium derived DEGs to genes with DPRB in proximity to identify genes whose transcription is likely regulated during the menstrual cycle by PGR. In total, we identified 653 such genes, and one of the top enriched pathways identified by gene set enrichment analysis was xenobiotic metabolism. Xenobiotics are conventionally defined as entities foreign to a cell or tissue, although it can also refer to entities found at levels greater than considered norm. Xenobiotic metabolism hence refers to the modification of these entities which in turn allows their systemic removal. Genes involved in this pathway are broadly categorized into 3 phases: phase 1 and phase 2 enzymes increase the solubility of the xenobiotics by introducing polar moieties and conjugating to endogenous hydrophilic molecules; and phase 3 genes encode transporters which then traffic the xenobiotic metabolites out of the cells to be excreted [63]. Although expression of xenobiotic metabolizing genes has been previously reported in the endometrium [64], defined and validated endometrial expression and function are still absent. Our data demonstrate transcriptional regulation of genes encoding phase 1 and 2 enzymes, as well as phase 3 transporters in the endometrium. These included numerous aldehyde dehydrogenase (ALDH) members, carboxylesterases, carbohydrate sulfotransferases, cytochrome P450 members, glutathione S-transferases, monoamine oxidases and UDP glycotransferases; and multi-drug resistance protein member ABCC3. Independent qPCR analysis confirmed that xenobiotic metabolism genes were indeed transcriptionally regulated during the menstrual cycle. Interestingly, genes encoding receptors known to mediate xenobiotic metabolism gene expression, including *NR1I3* and *NR1I2* were virtually not expressed (FPKM < 1), while *AHR* was

lowly abundant and non-differentially expressed in the endometrium during the phase transition (data not shown), suggesting that transcriptional regulation of the xenobiotic metabolism network may not occur in a classical manner, but rather through alternative regulatory mechanisms [65]. Whilst the impact of xenobiotic metabolism regulation during mid-secretory in the human endometrium remains elusive, there has been evidence linking dysregulation of xenobiotic metabolism genes to pathological conditions such as infertility and cancer [66]. Moreover, it has been proposed that xenobiotic metabolism may act as a detoxification mechanism, providing protection and guarding the endometrium against harmful environmental insult for appropriate and efficient implantation, such as environmental estrogen [66].

In addition to xenobiotic metabolism, apoptosis and EMT were also pathways identified as PGR regulated, and both have received ample attention as pathways important in endometrial function. Apoptosis has long been known to mediate uterine homeostasis, a disruption of which is evidently linked to implantation failure and endometriosis [67, 68]. Based on our *in silico* analysis, PGR appeared to promote as well as suppress apoptosis in the mid-secretory endometrium (See Supplemental Material 3). However, the onset of apoptosis in the cycling endometrium is typically around the late-secretory to menstruation phase [69], suggesting a possibility that during the MS phase, PGR acts to balance rather than induce cell death before the mass apoptosis ensues during late-secretory and menses. Indeed, we confirmed increased PGR binding and increased transcription of both pro- and anti-apoptotic genes including *EMP1* [70], *IER3* [71] and *BCL2L10* [72]. EMT and its reciprocal pathway, the mesenchymal-epithelial transition (MET) are important modulators of uterine physiology. During each menstrual cycle, the endometrium undergoes extensive remodeling which involves the building and shedding of the functional layer. The origin of the epithelial cells has long been under debate, with some evidence supporting MET being a major player for endometrial re-epithelialization [73, 74]. It has been postulated that by retaining

imprint of the mesenchymal origin, the endometrial epithelial cells are prone to return to its mesenchymal state via EMT [75]. In the MS endometrium, we found various EMT modulating genes to be transcriptionally regulated and possibly by PGR, including *MMP2*, *SERPINE1*, *NNMT*, and *WNT5A*. Interestingly, although PGR appeared to promote the expression of EMT genes during the WOI, a closer examination of our gene expression data actually suggests that the consequences of these regulatory activities resulted in neither decreased epithelial properties nor increased mesenchymal properties. The mesenchymal cell marker *CDH2* was strongly repressed (seven-fold), while another marker, *VIM*, although not identified as a DEG, showed a significant decrease with a fold-change that did not qualify for differential expression in the MS endometrium (data not shown). On the other hand, numerous epithelial cell markers including *CDH1*, *CLDN1*, *CLDN4*, *CLDN8*, *CLDN10*, *KLF4* and *KLF5* were all upregulated during MS. Additionally, *CLDN4*, *CLDN8* and *KLF4* were also presented with increased PGR binding in proximity, suggesting that PGR may directly promote the upregulation of these epithelial markers and maintain the epithelial-like characteristic of these cells. It is possible that while some mesenchymal properties in the epithelium provide for the implanting embryo (such as decreased cell to cell adhesion), but a complete loss of the epithelial status is likely unfavorable and hence PGR acts both to increase EMT as well as maintain the epithelial state. In support of this, EMT has been postulated as an important modulator of noninvasive trophoblast implantation in bovines [76].

Comparison of the upstream regulator activities for DEGs with and without differential PGR binding was attempted to further identify molecules with potential association with PGR. In this search, both FOXO1 and progesterone displayed increased activity in the regulation of DPRB DEGs, confirming that regulation of this group of genes was indeed associated with PGR activity [55]. Here, we identified various signaling factors Including NFKB proteins, the MET/HGF and fat

metabolism signaling modulators to show increased activity in regulating DEGs with DPRB, suggesting that PGR could be directly or indirectly regulating these pathways. Members of the NFKB family showed increased activity, suggesting a co-operative action with PGR. Whilst many studies have found PGR to exert an inhibitory effect on NFKB transcriptional activity [77, 78], *in silico* analysis of our gene expression datasets by IPA suggests that at least some members (REL, RELB and NFKB2) may engage in a cooperative relationship with PGR in regulating gene expression. Indeed, the observation of PGR's antagonizing impact on NFKB transcriptional activity is based primarily on p65 (RELA) [77, 79], and our analysis accordingly showed that RELA exhibited lower activity score in the regulation of DEGs with DPRB, compared to DEGs without DPRB (data not shown). Moreover, Hsu *et al*. showed that PGR isoform A, but not isoform B is required for NFKB nuclear translocation and subsequent p53 promoter activation in human umbilical venous endothelial cells [80]. These reports, together with our findings suggest that the interplay between PGR and NFKB proteins is sophisticated, relying on both PGR isoform as well as cell type. Furthermore, the nature of PGR- NFKB relationship may also be different for different NFKB members. Future studies aimed at assessing the association between NFKB and PGR should be examined and interpreted with caution. Lastly, dysregulation of the intracellular lipid regulator PLIN5 and mutation of the fat metabolism regulator LEPR are both associated with insulin resistance [81, 82], and PLIN5, LEPR and Insulin I were all found to be more active in regulating the DPRB DEGs, suggesting that PGR may indirectly regulate fat metabolism and insulin response through these factors. Indeed, our RNA-seq results demonstrated elevated levels of various insulin-regulated genes, confirming that the fat metabolism pathway is likely more activated in the DPRB DEGs.

Role and function of the endometrial epithelia during the WOI

RNA-seq was conducted to evaluate the transcriptomic profile in the epithelial compartment of the endometrium. A simple functional annotation found comparable biological functions as that of the whole endometrium, including inflammatory responses, TNFA/NFKB signaling, xenobiotic metabolism, apoptosis, KRAS signaling and EMT as positively enriched; and E2F signaling, G2M checkpoint, mitotic spindle and DNA repair as negatively enriched. To further unravel molecular pathways with increased specificity to the epithelium, we used two additional approaches. Firstly, we compared the whole endometrial-derived DEGs to epithelial-derived DEGs and excluded the common DEGs to obtain a profile of DEGs that were only detected in the epithelium. Whilst excluding the “common” DEGs may seem counter-intuitive, since the epithelium comprises a part of the endometrium and some “epithelial” genes with substantial transcriptional changes would surface when examined in the whole endometrium, thereby excluding the common DEGs would altogether eliminate those genes. However, the purpose of the epithelial specific examination is to identify previously “missed” epithelial-specific pathways (genes) when examining the endometrium as a whole. Genes in this category may show changes that are subtle but not necessarily less important in nature, and hence our approach of excluding the “common” DEGs. The second approach was to compare the activity status of the upstream regulators calculated for each set of DEGs and identify upstream regulators with enhanced activity in the epithelium. Using the IPA software to examine the 658 epithelial-specific DEGs, the most represented canonical pathways were dermatan sulfate, chondroitin sulfate and cholesterol biosynthesis. Dermatan and chondroitin sulfate are glycosaminoglycans found mostly in the skin, blood vessels and the heart valves [83]. They are known to regulate coagulation and wound repair, as well as recruit natural killer cells into the uterus during the reproductive cycle [84]. However, the specific, and possibly exclusive role of the endometrial epithelial cells in biosynthesis of these glycosaminoglycans has not yet been reported. On the other hand, progesterone has been

reported to inhibit the synthesis of cholesterol in the uterine epithelium of mice, and this has been postulated as a mechanism to block epithelial cell proliferation. Our data accordingly suggest that suppression of cholesterol biosynthesis may be more specifically refined to the epithelial compartment, possibly associated with PGR-mediated inhibition of epithelial cell proliferation during the MS phase [85].

Lastly, we identified two transcription factors, IRF8 and MEF2C with enhanced activity in the epithelium, whose protein levels and cellular localization were regulated in a compartment-specific way during the menstrual cycle. IRF8 (ICSBP) is a member of the interferon (IFN) regulatory factor (IRF) family and is known to regulate gene expression in an interferon-dependent manner [86]. It is a modulator of cellular apoptosis under pathological conditions and deregulation of other members of the family are associated with endometrial adenocarcinoma [87-91], suggesting that IRF proteins may indeed play important roles in the female reproductive tract. Supporting this, Kashiwagi *et al*. have reported IRF8 expression in the murine endometrium in response to the implanting embryo, but not in pseudopregnancy [92], and Kusama later reported the upregulation of IRF8 in the bovine endometrial luminal epithelium in response to the embryo derived interferon tau [93]. On the other hand, MEF2C belongs to the MADS box transcription enhancer 2 family, which plays a role in proliferation, invasion and differentiation in various cell types [94]. Other members of the family (MEF2A and MEF2D) are known to modulate cytotrophoblast invasion and differentiation in the human placenta [95], and MEF2C itself has been associated with endometriosis, although no apparent function has been reported in the endometrial epithelium [96]. Whilst very little is known regarding the epithelial function of IRF8 and MEF2C in the endometrium during the WOI, our findings suggest that these factors could have important functions in the uterus and female reproduction.

In summary, signaling pathways controlled by progesterone and PGR are indispensable in uterine biology and homeostasis, a disruption of which manifests in a wide range of gynecological abnormalities such as endometriosis, adenomyosis, fertility defects and endometrial cancer. These pathological conditions are linked to dysregulation of many molecular pathways amongst which are EMT, apoptosis, cell migration and inflammatory response. In this study we provide evidence to show how some of these pathways could be directly controlled by the progesterone signaling pathway through the transcriptional activity of PGR. An understanding of the precise regulatory pattern and mechanism of PGR, that is, what genes are regulated by PGR, and how these genes are regulated by PGR provide a bridging link to explain the molecular mechanism of disease phenotypes under aberrantly regulated PGR conditions. One limitation of this study is that ChIP-seq cannot take into consideration the control of PGR over distal DNA response element due to the chromatin interaction in a three-dimensional structure. To address this, future studies should aim to attain a comprehensive three-dimensional structure to elucidate the chromatin conformation in parallel to PGR binding using techniques such as Hi-C [97, 98]. This will allow the identification of PGR binding sites in a more global view without the limitation of chromosomal distance. Additional to the PGR regulatory function, approaching the uterine transcriptomic analysis in a compartment specific manner enabled the identification of numerous proteins with previously unrecognized roles in uterine biology and pregnancy. These findings provide a direction for future studies aimed to explore molecular factors crucial for uterine homeostasis.

Materials and Methods

Ethics Statement

This project was executed in accordance with the federal regulation governing human subject research. All procedures were approved by the following ethics committees the University of North Carolina at Chapel Hill IRB under file #:05-1757. Informed consent was obtained from all patients before their participation in this study.

Human Endometrial Samples

We recruited normal volunteers with the following inclusion criteria: ages 18-37, normal menstrual cycle characteristics, an inter-cycle interval of 25-35 days, varying no more than 2 days from cycle to cycle, a normal luteal phase length without luteal spotting, and a body mass index (BMI) between 19 - 28. We excluded women with infertility, pelvic pain, signs and symptoms of endometriosis, history of fibroids or history of taking medication affecting hormonal function in the last 3 months. Endometrial samples were taken using an office biopsy instrument (Pipelle™, Milex Products Inc., Chicago, IL) from healthy, reproductive-aged, normally cycling women with no history of infertility or other gynecological disease. Cycle day was determined based on the last menstrual period combined with menstrual history (P samples) or date of Luteinizing Hormone surge. Cycle phase and endometrial normality was confirmed with H&E staining based on the Noyes criteria [99].

RNA-seq and Analysis

The RNA was prepared from endometrial samples using TRIzol (Thermo Fisher Scientific, Waltham, MA) under the manufacturer's suggested conditions. Absorption spectroscopy (NanoDrop 8000, Thermo Fisher Scientific, Waltham, MA) was used for quantification of RNA with a ribosomal RNA standard curve. The RNA libraries were sequenced with a HiSeq 2000 system (Illumina). The raw RNA-Seq reads (100 nt, paired-end) were initially processed by filtering with average quality scores greater than 20. Reads which passed the initial processing were aligned to the human reference genome (hg19; Genome Reference Consortium Human Build 19 from February 2009) using TopHat version 2.0.4 [100] and assembled using Cufflinks version 2.0.2 [101]. BigWig file was generated from normalized bedgraph file of each sample using bedGraphToBigWig. Scores represent normalized mapped read coverage. Expression values of RNA-Seq were expressed as FPKM (fragments per kilobase of exon per million fragments) values. Differential expression was calculated using Cuffdiff [101]. Transcripts with FPKM > 1, *q*-value < 0.05 and at least 1.5-fold change were defined as differentially expressed genes (DEG). The data discussed in this publication have been deposited in NCBI's Gene Expression Omnibus and are accessible through GEO Series accession number GSE132713 (https://www.ncbi.nlm.nih.gov/geo/query/acc.cgi?acc=GSE132713).

Chromatin immunoprecipitation sequencing (ChIP-seq) and qRT-PCR (ChIP-qPCR)

Endometrial tissues were flash frozen and sent to the Active Motif company for Factor-Path ChIP-seq analysis. The tissues were fixed, followed by sonication to shear the chromatin into smaller fragments before immunoprecipitation using the Progesterone Receptor (PGR) antibody (sc-7208, Santa Cruz). PGR-bound DNA was subsequently purified and amplified to generate a library for sequencing and quantitative real-time PCR (ChIP-seq and ChIP-qPCR). Sequencing was performed using a HiSeq 2000 system (Illumina). The raw ChIP-seq reads (75 nt, single-end) were processed and aligned to the human reference genome (hg19; Genome Reference

Consortium Human Build 19 from February 2009) using Bowtie version 1.1.2 [102] with unique mapping and up to 2 mismatches for each read (-m 1 -v 2). The duplicated reads with the same sequence were discarded. The bigWig files were displayed on UCSC genome browser as custom tracks. Peak calling for each sample was performed by SICER version 1.1 with FDR of 0.001. Software MEDIP was used to identify differential peaks of PGR binding between the P and MS samples [103]. Each region was defined as the genomic interval with at least 2-fold difference of read count and *p*-value ≤ 0.01. Each differential peak was mapped to nearby gene using software HOMER's "annotatePeaks.pl" function [104]. The motif analysis of differential PGR binding peaks was performed using HOMER software's "findMotifsGenome.pl" command with default setting [104]. The data discussed in this publication have been deposited in NCBI's Gene Expression Omnibus and are accessible through GEO Series accession number GSE132713 (https://www.ncbi.nlm.nih.gov/geo/query/acc.cgi?acc=GSE132713).

Epithelial isolation

Endometrial samples obtained from normal controls during the secretory phase of the menstrual cycle were washed with Opti-mem media supplemented with fetal bovine serum (FBS) and antibiotics (10 000 IU/mL penicillin, 10 000 IU/ mL streptomycin; Life Technologies, Grand Island, New York). Tissue was recovered via centrifugation and incubated with collagenase-containing medium (phenol red-free Dul- becco Modified Eagle Medium/F12, 0.5% collagenase I, 0.02% DNase, and 5% FBS). Cell types were separated as described previously [105].

RNA extraction, cDNA conversion and qPCR

For validation of RNA-seq results, selected genes were examined for RNA expression using independent patients' samples. Endometrial tissues were resected from patients and flash frozen

652 in liquid nitrogen. RNA was extracted as described above. Reverse transcription was performed
653 to convert RNA into cDNA using the Moloney Murine Leukemia Virus (MMLV) reverse
654 transcriptase (Thermo Fisher) according to the manufacturer's instructions. Quantitative real-time
655 PCR was performed using the SsoAdvancedTM Universal SYBR Green Supermix (1725274, Bio-
656 Rad). Briefly, reaction samples were prepared to a total volume of 10 µL with 250 nM of each of
657 the forward and reverse primers, 0.5 ng of cDNA and a final 1 X concentration of the SYBR Green
658 Supermix. The reaction was heated to 98 ^{O}C for 30 sec, followed by 35 cycles of denaturation at
659 95 ^{O}C for 5 sec and annealing and elongation for 15 sec. Temperature cycles were performed on
660 the CFX Connect^{TM} Real-Time PCR Detection System (Bio-Rad). The primer sequences were as
661 follows (from 5' to 3', F = forward and R = reverse): *CYP3A5* - GTATGAAGGTCAACTCCCTGTG
662 (F) and GGGCCTAAAGACCTTCGATTT (R); *FMO5* - GATTTAAGACCACTGTGTGCAG (F),
663 CCATGACTCCATCAAAGACATTC (R); *UGT1A6* – TGTCTCAGGAATTTGAAGCCTAC (F),
664 GCAATTGCCATAGCTTTCTTCTC (R); *SLCO4A1* – CCCGTCTACATTGCCATCTT (F),
665 GGCCCATTTCCGTGTAGATATT (R); *SLC6A12* – CTTCTACCTGTTCAGCTCCTTC (F),
666 CGTGCAATGCTCTGTGTTC (R); *CYP2C18* – CATTGTGGTGTTGCATGGATATG (F),
667 AGGATTCCAAGTCCTTTGTTAACTT (R); *SULT1C4* – TAAAGCAGGAACAACATGGACT (F),
668 TTCGAGGAAAGGAAATCGTTGA (R); *SLCO2A1* – CTGTACAGCGCCTACTTCAA (F),
669 GATGGCATTGCTGATCTCATTC (R); *GSTM1* – CAAGCACAACCTGTGTGG (F),
670 TTGTCCATGGTCTGGTTCTC (R); *GSTM3* – GGAGTTCACGGATACCTCTTATG (F),
671 GGTAGGGCAGATTAGGAAAGTC (R); *GSTM5* – CGCTTTGAGGGTTTGAAGAAG (F),
672 TGGGCCCTATTTGCTGTT (R); *EMP1* – GTCTTCGTGTTCCAGCTCTT (F),
673 AAGAATGCACAGCCAGCA (R); *IER3* – TGGAACTGCGGCAAAGTA (F),
674 GTAGACAGACGGAGTTGAGATG (R); *BCL2L10* – CCAAAGAACCGCAGAAGAAAC (F),
675 GAAGTTGTGGAGAGATGAGAGG (R); *GPX3* – TCTGGTCATTCTGGGCTTTC (F),
676 ACCTGGTCGGACATACTTGA (R); *TIMP3* – CCCATGTGCAGTACATCCATAC (F),
677 ATCATAGACGCGACCTGTCA (R); *VNN1* – CAGATCAGGGTGCGCATATT (F),

GTTTACTTCAGGGTCTGGGATG (R); *SERPINE1* – CTGAGAACTTCAGGATGCAGAT (F), AGACCCTTCACCAAAGACAAG (R); *NNMT* – ACCTCCAAGGACACCTATCT (F), CACACCGTCTAGGCAGAATATC (R); and *TGM2* – ACCCAGCAGGGCTTTATCTA (F), CCCATCTTCAAACTGCCCAA (R). All primers were synthesized by Sigma-Aldrich (St Louis, MO), and gene expression was normalized to 18s rRNA by ΔΔCT method.

Immunohistochemistry

Sections were cut from patient's endometrial biopsies that have been formalin-fixed and paraffin embedded at 5 µm per section. Sections were baked at 65°C for roughly 5 minutes and deparaffined using the Citrisolv clearing agent (22-143-975, Thermo Fisher, Waltham, MA, USA) and hydrated by immersing in decreasing gradient of ethanol. Antigen retrieval was performed using the Vector Labs Antigen Unmasking Solution as per manufacturer's protocol (H-3300, Vector Laboratories, Burlingame, CA, USA), followed by blocking the endogenous peroxide using 3% hydrogen peroxide diluted in distilled water. The tissue was blocked in 5% normal donkey serum before an overnight incubation with the primary antibody at 4°C (1:200 for ICSBP antibody, sc-365042, Santa Cruz; and 1:100 for MEF2C antibody, SAB4501860, Sigma-Aldrich). The slides were washed twice in PBS at room temperature and applied with secondary antibody diluted 1:200 in 1% BSA prepared in PBS (biotinylated anti-mouse IgG (H+L), BA-9200, and biotinylated anti-rabbit IgG (H+L), BA-1000, Vector Laboratories). The ABC reagent was applied to tissue in accordance with the manufacturer's instructions (Vector Labs ABC PK-6100, Vector Laboratories). Signal was developed using the Vector Labs DAB ImmPACT staining kit (Vector Labs SK-4105, Vector Laboratories). Finally, the tissue sections were counterstained with hematoxylin and dehydrated through increasing ethanol concentration before incubation in Citrisolv and coverslipping.

Data Analysis

Various bioinformatic tools were utilized to analyze the high content data generated in this study. Principle component analysis and hierarchical clustering were achieved using the Partek Genomics Suites 7.0 (Partek Inc., St. Louis, MO, USA, http://www.partek.com/partek-genomics-suite/). Functional annotation and enrichment analysis were performed using a combination of the following three tools: Ingenuity Pathway Analysis Software (IPA, http://www.ingenuity.com/), Gene Set Enrichment Analysis (GSEA, http://software.broadinstitute.org/gsea/index.jsp/), and Database for Annotation, Visualization and Integrated Discovery (DAVID, http://david.ncifcrf.gov/). Distribution of PGR binding throughout the genome was conducted using the Peak Annotation and Visualization tool (PAVIS, https://manticore.niehs.nih.gov/pavis2/) [106], and PGR-bound motif was submitted to HOMER motif analysis software to identify presence of other DNA-response elements (http://homer.salk.edu/homer/). GraphPad Prism software was used to analyze single gene expression data generated from both RNA-seq, qPCR, and PGR ChIP-qPCR. Statistical analysis including one-way ANOVA and Student's *t* test, with a *p*-value of less than 0.05 considered as significant. For pathway analysis using IPA, a given biological category was subjected to Fisher's exact test to measure the probability that the category was randomly associated. The categories with *p*-values less than 0.05 were defined as significantly enriched.

References

1. Paiva, P., et al., *Human chorionic gonadotrophin regulates FGF2 and other cytokines produced by human endometrial epithelial cells, providing a mechanism for enhancing endometrial receptivity.* Hum Reprod, 2011. **26**(5): p. 1153-62.
2. Gellersen, B. and J.J. Brosens, *Cyclic decidualization of the human endometrium in reproductive health and failure.* Endocr Rev, 2014. **35**(6): p. 851-905.
3. Jabbour, H.N., et al., *Endocrine regulation of menstruation.* Endocr Rev, 2006. **27**(1): p. 17-46.
4. Ramathal, C.Y., et al., *Endometrial decidualization: of mice and men.* Semin Reprod Med, 2010. **28**(1): p. 17-26.
5. Hawkins, S.M. and M.M. Matzuk, *Menstrual Cycle: Basic Biology.* Ann N Y Acad Sci, 2008. **1135**: p. 10-8.
6. Mesen, T.B. and S.L. Young, *Progesterone and the luteal phase: a requisite to reproduction.* Obstet Gynecol Clin North Am, 2015. **42**(1): p. 135-51.
7. Speroff, L. and M.A. Fritz, *Clinical Gynecologic Endocrinology and Infertility*. 2005: Lippincott Williams & Wilkins.
8. Bashiri, A., K.I. Halper, and R. Orvieto, *Recurrent Implantation Failure-update overview on etiology, diagnosis, treatment and future directions.* Reprod Biol Endocrinol, 2018. **16**(1): p. 121.
9. Simon, A. and N. Laufer, *Assessment and treatment of repeated implantation failure (RIF).* J Assist Reprod Genet, 2012. **29**(11): p. 1227-39.
10. Garrido-Gomez, T., et al., *Defective decidualization during and after severe preeclampsia reveals a possible maternal contribution to the etiology.* Proc Natl Acad Sci U S A, 2017. **114**(40): p. E8468-e8477.
11. Conrad, K.P., M.B. Rabaglino, and E.D. Post Uiterweer, *Emerging role for dysregulated decidualization in the genesis of preeclampsia.* Placenta, 2017. **60**: p. 119-129.
12. Macklon, N.S., J.P. Geraedts, and B.C. Fauser, *Conception to ongoing pregnancy: the 'black box' of early pregnancy loss.* Hum Reprod Update, 2002. **8**(4): p. 333-43.
13. Dey, S.K., et al., *Molecular cues to implantation.* Endocr Rev, 2004. **25**(3): p. 341-73.
14. Bhurke, A.S., I.C. Bagchi, and M.K. Bagchi, *Progesterone-Regulated Endometrial Factors Controlling Implantation.* Am J Reprod Immunol, 2016. **75**(3): p. 237-45.
15. Pawar, S., et al., *Minireview: Steroid-regulated paracrine mechanisms controlling implantation.* Mol Endocrinol, 2014. **28**(9): p. 1408-22.
16. Young, S.L., *Oestrogen and progesterone action on endometrium: a translational approach to understanding endometrial receptivity.* Reprod Biomed Online, 2013. **27**(5): p. 497-505.
17. Young, S.L., et al., *Effect of randomized serum progesterone concentration on secretory endometrial histologic development and gene expression.* Hum Reprod, 2017. **32**(9): p. 1903-1914.
18. Wilcox, A.J., D.D. Baird, and C.R. Weinberg, *Time of implantation of the conceptus and loss of pregnancy.* N Engl J Med, 1999. **340**(23): p. 1796-9.
19. Sunderam, S., et al., *Assisted reproductive technology surveillance--United States, 2009.* MMWR Surveill Summ, 2012. **61**(7): p. 1-23.
20. Prapas, Y., et al., *The window for embryo transfer in oocyte donation cycles depends on the duration of progesterone therapy.* Hum Reprod, 1998. **13**(3): p. 720-3.
21. Patel, B., et al., *Role of nuclear progesterone receptor isoforms in uterine pathophysiology.* Hum Reprod Update, 2015. **21**(2): p. 155-73.

765 22. Yin, P., et al., *Genome-wide progesterone receptor binding: cell type-specific and shared*
766 *mechanisms in T47D breast cancer cells and primary leiomyoma cells.* PLoS One, 2012. **7**(1): p.
767 e29021.
768 23. Kim, J.J., T. Kurita, and S.E. Bulun, *Progesterone action in endometrial cancer, endometriosis,*
769 *uterine fibroids, and breast cancer.* Endocr Rev, 2013. **34**(1): p. 130-62.
770 24. Tamm, K., et al., *Genes targeted by the estrogen and progesterone receptors in the human*
771 *endometrial cell lines HEC1A and RL95-2.* Reprod Biol Endocrinol, 2009. **7**: p. 150.
772 25. Ingamells, S., et al., *Endometrial progesterone receptor expression during the human menstrual*
773 *cycle.* J Reprod Fertil, 1996. **106**(1): p. 33-8.
774 26. Matsumoto, H., et al., *Indian hedgehog as a progesterone-responsive factor mediating*
775 *epithelial-mesenchymal interactions in the mouse uterus.* Dev Biol, 2002. **245**(2): p. 280-90.
776 27. Takamoto, N., et al., *Identification of Indian hedgehog as a progesterone-responsive gene in the*
777 *murine uterus.* Mol Endocrinol, 2002. **16**(10): p. 2338-48.
778 28. Franco, H.L., et al., *Epithelial progesterone receptor exhibits pleiotropic roles in uterine*
779 *development and function.* Faseb j, 2012. **26**(3): p. 1218-27.
780 29. Pan, H., et al., *Microarray analysis of uterine epithelial gene expression during the implantation*
781 *window in the mouse.* Endocrinology, 2006. **147**(10): p. 4904-16.
782 30. Mazur, E.C., et al., *Progesterone receptor transcriptome and cistrome in decidualized human*
783 *endometrial stromal cells.* Endocrinology, 2015. **156**(6): p. 2239-53.
784 31. Li, Q., et al., *The antiproliferative action of progesterone in uterine epithelium is mediated by*
785 *Hand2.* Science, 2011. **331**(6019): p. 912-6.
786 32. Lee, K.Y., et al., *Bmp2 is critical for the murine uterine decidual response.* Mol Cell Biol, 2007.
787 **27**(15): p. 5468-78.
788 33. Li, Q., et al., *Bone morphogenetic protein 2 functions via a conserved signaling pathway*
789 *involving Wnt4 to regulate uterine decidualization in the mouse and the human.* J Biol Chem,
790 2007. **282**(43): p. 31725-32.
791 34. Lim, H., et al., *Hoxa-10 regulates uterine stromal cell responsiveness to progesterone during*
792 *implantation and decidualization in the mouse.* Mol Endocrinol, 1999. **13**(6): p. 1005-17.
793 35. Taylor, H.S., et al., *HOXA10 is expressed in response to sex steroids at the time of implantation in*
794 *the human endometrium.* J Clin Invest, 1998. **101**(7): p. 1379-84.
795 36. Kannan, A., et al., *The transcription factor C/EBPbeta is a marker of uterine receptivity and*
796 *expressed at the implantation site in the primate.* Reprod Sci, 2010. **17**(5): p. 434-43.
797 37. Mantena, S.R., et al., *C/EBPbeta is a critical mediator of steroid hormone-regulated cell*
798 *proliferation and differentiation in the uterine epithelium and stroma.* Proc Natl Acad Sci U S A,
799 2006. **103**(6): p. 1870-5.
800 38. Plante, B.J., et al., *Cyclic regulation of transcription factor C/EBP beta in human endometrium.*
801 Reprod Biol Endocrinol, 2009. **7**: p. 15.
802 39. Gray, C.A., et al., *Developmental biology of uterine glands.* Biol Reprod, 2001. **65**(5): p. 1311-23.
803 40. Kelleher, A.M., F.J. DeMayo, and T.E. Spencer, *Uterine Glands: Developmental Biology and*
804 *Functional Roles in Pregnancy.* Endocr Rev, 2019.
805 41. Singh, H. and J.D. Aplin, *Adhesion molecules in endometrial epithelium: tissue integrity and*
806 *embryo implantation.* J Anat, 2009. **215**(1): p. 3-13.
807 42. Wang, B., et al., *Annexin A2 Acts as an Adhesion Molecule on the Endometrial Epithelium during*
808 *Implantation in Mice.* PLoS One, 2015. **10**(10): p. e0139506.
809 43. Guffanti, E., et al., *Nuclear pore complex proteins mark the implantation window in human*
810 *endometrium.* J Cell Sci, 2008. **121**(Pt 12): p. 2037-45.
811 44. Salker, M.S., et al., *Activation of SGK1 in Endometrial Epithelial Cells in Response to PI3K/AKT*
812 *Inhibition Impairs Embryo Implantation.* Cell Physiol Biochem, 2016. **39**(5): p. 2077-2087.

813 45. Boeddeker, S.J. and A.P. Hess, *The role of apoptosis in human embryo implantation.* J Reprod
814 Immunol, 2015. **108**: p. 114-22.
815 46. Joswig, A., et al., *Apoptosis in uterine epithelium and decidua in response to implantation:*
816 *evidence for two different pathways.* Reprod Biol Endocrinol, 2003. **1**: p. 44.
817 47. Valdez-Morales, F.J., et al., *Changes in receptivity epithelial cell markers of endometrium after*
818 *ovarian stimulation treatments: its role during implantation window.* Reprod Health, 2015. **12**: p.
819 45.
820 48. Kelleher, A.M., et al., *Uterine glands coordinate on-time embryo implantation and impact*
821 *endometrial decidualization for pregnancy success.* Nat Commun, 2018. **9**(1): p. 2435.
822 49. Aghajanova, L., *Leukemia inhibitory factor and human embryo implantation.* Ann N Y Acad Sci,
823 2004. **1034**: p. 176-83.
824 50. Kimber, S.J., *Leukaemia inhibitory factor in implantation and uterine biology.* Reproduction,
825 2005. **130**(2): p. 131-45.
826 51. Norwitz, E.R., D.J. Schust, and S.J. Fisher, *Implantation and the survival of early pregnancy.* N
827 Engl J Med, 2001. **345**(19): p. 1400-8.
828 52. Vassen, L., W. Wegrzyn, and L. Klein-Hitpass, *Human insulin receptor substrate-2 (IRS-2) is a*
829 *primary progesterone response gene.* Mol Endocrinol, 1999. **13**(3): p. 485-94.
830 53. Kaya, H.S., et al., *Roles of progesterone receptor A and B isoforms during human endometrial*
831 *decidualization.* Mol Endocrinol, 2015. **29**(6): p. 882-95.
832 54. Okada, H., T. Tsuzuki, and H. Murata, *Decidualization of the human endometrium.* Reprod Med
833 Biol, 2018. **17**(3): p. 220-227.
834 55. Vasquez, Y.M., et al., *FOXO1 is required for binding of PR on IRF4, novel transcriptional regulator*
835 *of endometrial stromal decidualization.* Mol Endocrinol, 2015. **29**(3): p. 421-33.
836 56. Rubel, C.A., et al., *A Gata2-Dependent Transcription Network Regulates Uterine Progesterone*
837 *Responsiveness and Endometrial Function.* Cell Rep, 2016. **17**(5): p. 1414-1425.
838 57. Wang, X., et al., *SOX17 regulates uterine epithelial-stromal cross-talk acting via a distal enhancer*
839 *upstream of Ihh.* Nat Commun, 2018. **9**(1): p. 4421.
840 58. Huang da, W., B.T. Sherman, and R.A. Lempicki, *Bioinformatics enrichment tools: paths toward*
841 *the comprehensive functional analysis of large gene lists.* Nucleic Acids Res, 2009. **37**(1): p. 1-13.
842 59. Huang da, W., B.T. Sherman, and R.A. Lempicki, *Systematic and integrative analysis of large*
843 *gene lists using DAVID bioinformatics resources.* Nat Protoc, 2009. **4**(1): p. 44-57.
844 60. Subramanian, A., et al., *Gene set enrichment analysis: a knowledge-based approach for*
845 *interpreting genome-wide expression profiles.* Proc Natl Acad Sci U S A, 2005. **102**(43): p. 15545-
846 50.
847 61. Owen, G.I., et al., *Progesterone regulates transcription of the p21(WAF1) cyclin- dependent*
848 *kinase inhibitor gene through Sp1 and CBP/p300.* J Biol Chem, 1998. **273**(17): p. 10696-701.
849 62. Tseng, L., et al., *Progesterone receptor (hPR) upregulates the fibronectin promoter activity in*
850 *human decidual fibroblasts.* DNA Cell Biol, 2003. **22**(10): p. 633-40.
851 63. Omiecinski, C.J., et al., *Xenobiotic metabolism, disposition, and regulation by receptors: from*
852 *biochemical phenomenon to predictors of major toxicities.* Toxicol Sci, 2011. **120 Suppl 1**: p. S49-
853 75.
854 64. Tseng, L.H., et al., *Genome-based expression profiling as a single standardized microarray*
855 *platform for the diagnosis of endometrial disorder: an array of 126-gene model.* Fertil Steril,
856 2010. **94**(1): p. 114-9.
857 65. Hariparsad, N., et al., *Identification of pregnane-X receptor target genes and coactivator and*
858 *corepressor binding to promoter elements in human hepatocytes.* Nucleic Acids Res, 2009. **37**(4):
859 p. 1160-73.

860 66. Altmae, S., et al., *Endometrial gene expression analysis at the time of embryo implantation in*
861 *women with unexplained infertility.* Mol Hum Reprod, 2010. **16**(3): p. 178-87.
862 67. Harada, T., et al., *Apoptosis in human endometrium and endometriosis.* Hum Reprod Update,
863 2004. **10**(1): p. 29-38.
864 68. Antsiferova, Y. and N. Sotnikova, *Apoptosis and endometrial receptivity: Relationship with in*
865 *vitro fertilization treatment outcome.* World Journal of Obstetrics and Gynecology, 2016. **5**(1): p.
866 87-96.
867 69. Kokawa, K., T. Shikone, and R. Nakano, *Apoptosis in the human uterine endometrium during the*
868 *menstrual cycle.* J Clin Endocrinol Metab, 1996. **81**(11): p. 4144-7.
869 70. Li, H., et al., *The expression and function of epithelial membrane protein 1 in laryngeal*
870 *carcinoma.* Int J Oncol, 2017. **50**(1): p. 141-148.
871 71. Akilov, O.E., et al., *Resistance of Sezary cells to TNF-alpha-induced apoptosis is mediated in part*
872 *by a loss of TNFR1 and a high level of the IER3 expression.* Exp Dermatol, 2012. **21**(4): p. 287-92.
873 72. Opferman, J.T. and A. Kothari, *Anti-apoptotic BCL-2 family members in development.* Cell Death
874 Differ, 2018. **25**(1): p. 37-45.
875 73. Maybin, J.A. and H.O. Critchley, *Menstrual physiology: implications for endometrial pathology*
876 *and beyond.* Hum Reprod Update, 2015. **21**(6): p. 748-61.
877 74. Bilyk, O., et al., *Epithelial-to-Mesenchymal Transition in the Female Reproductive Tract: From*
878 *Normal Functioning to Disease Pathology.* Front Oncol, 2017. **7**: p. 145.
879 75. Matsuzaki, S. and C. Darcha, *Epithelial to mesenchymal transition-like and mesenchymal to*
880 *epithelial transition-like processes might be involved in the pathogenesis of pelvic endometriosis.*
881 Hum Reprod, 2012. **27**(3): p. 712-21.
882 76. Bai, R., et al., *Down-regulation of transcription factor OVOL2 contributes to epithelial-*
883 *mesenchymal transition in a noninvasive type of trophoblast implantation to the maternal*
884 *endometrium.* Faseb j, 2018: p. fj201701131RR.
885 77. Hardy, D.B., et al., *Progesterone receptor plays a major antiinflammatory role in human*
886 *myometrial cells by antagonism of nuclear factor-kappaB activation of cyclooxygenase 2*
887 *expression.* Mol Endocrinol, 2006. **20**(11): p. 2724-33.
888 78. Davies, S., et al., *Identification of a novel mechanism of NF-kappaB inactivation by progesterone*
889 *through progesterone receptors in Hec50co poorly differentiated endometrial cancer cells:*
890 *induction of A20 and ABIN-2.* Gynecol Oncol, 2004. **94**(2): p. 463-70.
891 79. Kalkhoven, E., et al., *Negative interaction between the RelA(p65) subunit of NF-kappaB and the*
892 *progesterone receptor.* J Biol Chem, 1996. **271**(11): p. 6217-24.
893 80. Hsu, S.P., et al., *Progesterone receptor-NFkappaB complex formation is required for*
894 *progesterone-induced NFkappaB nuclear translocation and binding onto the p53 promoter.*
895 Endocrinology, 2015. **156**(1): p. 291-300.
896 81. Chiu, K.C., et al., *Association of leptin receptor polymorphism with insulin resistance.* Eur J
897 Endocrinol, 2004. **150**(5): p. 725-9.
898 82. Mason, R.R., et al., *PLIN5 deletion remodels intracellular lipid composition and causes insulin*
899 *resistance in muscle.* Mol Metab, 2014. **3**(6): p. 652-63.
900 83. Trowbridge, J.M. and R.L. Gallo, *Dermatan sulfate: new functions from an old*
901 *glycosaminoglycan.* Glycobiology, 2002. **12**(9): p. 117r-25r.
902 84. Kitaya, K. and T. Yasuo, *Regulatory role of membrane-bound form interleukin-15 on human*
903 *uterine microvascular endothelial cells in circulating CD16(-) natural killer cell extravasation into*
904 *human endometrium.* Biol Reprod, 2013. **89**(3): p. 70.
905 85. Stacey, K., et al., *Effects of female sex hormones on lipid metabolism in the uterine epithelium of*
906 *the mouse.* Int J Biochem, 1991. **23**(3): p. 371-6.

907 86. Tailor, P., et al., *The feedback phase of type I interferon induction in dendritic cells requires*
908 *interferon regulatory factor 8.* Immunity, 2007. **27**(2): p. 228-39.
909 87. Hu, X., et al., *IRF8 regulates acid ceramidase expression to mediate apoptosis and suppresses*
910 *myelogeneous leukemia.* Cancer Res, 2011. **71**(8): p. 2882-91.
911 88. Liu, K. and S.I. Abrams, *Coordinate regulation of IFN consensus sequence-binding protein and*
912 *caspase-1 in the sensitization of human colon carcinoma cells to Fas-mediated apoptosis by IFN-*
913 *gamma.* J Immunol, 2003. **170**(12): p. 6329-37.
914 89. Yang, D., et al., *Repression of IFN regulatory factor 8 by DNA methylation is a molecular*
915 *determinant of apoptotic resistance and metastatic phenotype in metastatic tumor cells.* Cancer
916 Res, 2007. **67**(7): p. 3301-9.
917 90. Giatromanolaki, A., et al., *Interferon regulatory factor-1 (IRF-1) suppression and derepression*
918 *during endometrial tumorigenesis and cancer progression.* Cytokine, 2004. **26**(4): p. 164-8.
919 91. Kuroboshi, H., et al., *Interferon regulatory factor-1 expression in human uterine endometrial*
920 *carcinoma.* Gynecol Oncol, 2003. **91**(2): p. 354-8.
921 92. Kashiwagi, A., et al., *The Postimplantation Embryo Differentially Regulates Endometrial Gene*
922 *Expression and Decidualization.* Endocrinology, 2007. **148**(9): p. 4173-4184.
923 93. Kusama, K., et al., *Endometrial factors similarly induced by IFNT2 and IFNTc1 through*
924 *transcription factor FOXS1.* PLoS One, 2017. **12**(2): p. e0171858.
925 94. Pon, J.R. and M.A. Marra, *MEF2 transcription factors: developmental regulators and emerging*
926 *cancer genes.* Oncotarget, 2016. **7**(3): p. 2297-312.
927 95. Li, L., L.P. Rubin, and X. Gong, *MEF2 transcription factors in human placenta and involvement in*
928 *cytotrophoblast invasion and differentiation.* Physiol Genomics, 2018. **50**(1): p. 10-19.
929 96. Ohlsson Teague, E.M., et al., *MicroRNA-regulated pathways associated with endometriosis.* Mol
930 Endocrinol, 2009. **23**(2): p. 265-75.
931 97. de Wit, E. and W. de Laat, *A decade of 3C technologies: insights into nuclear organization.* Genes
932 Dev, 2012. **26**(1): p. 11-24.
933 98. Diaz, N., et al., *Chromatin conformation analysis of primary patient tissue using a low input Hi-C*
934 *method.* Nat Commun, 2018. **9**(1): p. 4938.
935 99. Noyes, R.W., A.T. Hertig, and J. Rock, *Dating the endometrial biopsy.* Am J Obstet Gynecol, 1975.
936 **122**(2): p. 262-3.
937 100. Trapnell, C., L. Pachter, and S.L. Salzberg, *TopHat: discovering splice junctions with RNA-Seq.*
938 Bioinformatics, 2009. **25**(9): p. 1105-11.
939 101. Trapnell, C., et al., *Transcript assembly and quantification by RNA-Seq reveals unannotated*
940 *transcripts and isoform switching during cell differentiation.* Nat Biotechnol, 2010. **28**(5): p. 511-
941 5.
942 102. Langmead, B., et al., *Ultrafast and memory-efficient alignment of short DNA sequences to the*
943 *human genome.* Genome Biol, 2009. **10**(3): p. R25.
944 103. Zang, C., et al., *A clustering approach for identification of enriched domains from histone*
945 *modification ChIP-Seq data.* Bioinformatics, 2009. **25**(15): p. 1952-8.
946 104. Heinz, S., et al., *Simple combinations of lineage-determining transcription factors prime cis-*
947 *regulatory elements required for macrophage and B cell identities.* Mol Cell, 2010. **38**(4): p. 576-
948 89.
949 105. Arnold, J.T., et al., *Endometrial stromal cells regulate epithelial cell growth in vitro: a new co-*
950 *culture model.* Hum Reprod, 2001. **16**(5): p. 836-45.
951 106. Huang, W., et al., *PAVIS: a tool for Peak Annotation and Visualization.* Bioinformatics, 2013.
952 **29**(23): p. 3097-9.

953

FIGURES

Figure 1.

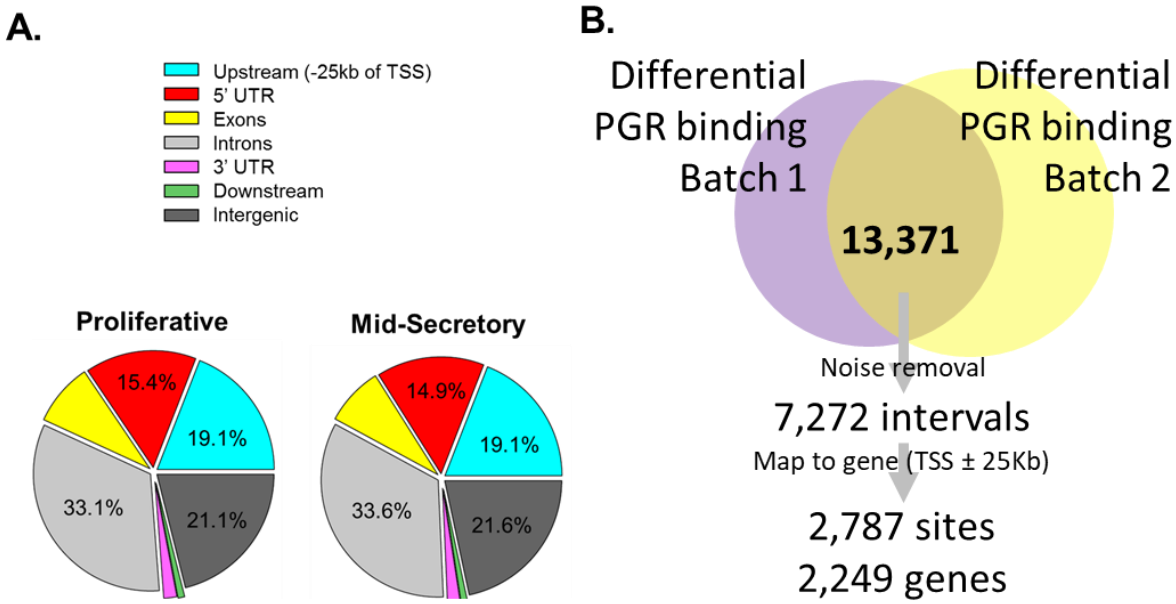

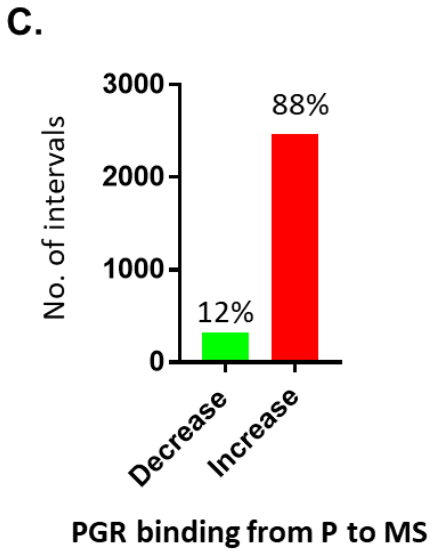

D.

Category	% of genes	p-value
Cell migration	7.6	6.40E-11
Regulation of signal transduction	14.7	8.20E-11
Angiogenesis	3.3	7.20E-09
Vasculature development	4.3	9.10E+09
Cardiovascular system development	6	1.00E-08
Circulatory system development	6	1.00E-08
Blood vessel development	4.1	2.00E-08
Regulation of intracellular signal transduction	9.4	9.10E-08
Regulation of cell migration	4.6	9.60E-08
Secretion	6.5	1.90E-07

Figure 2.

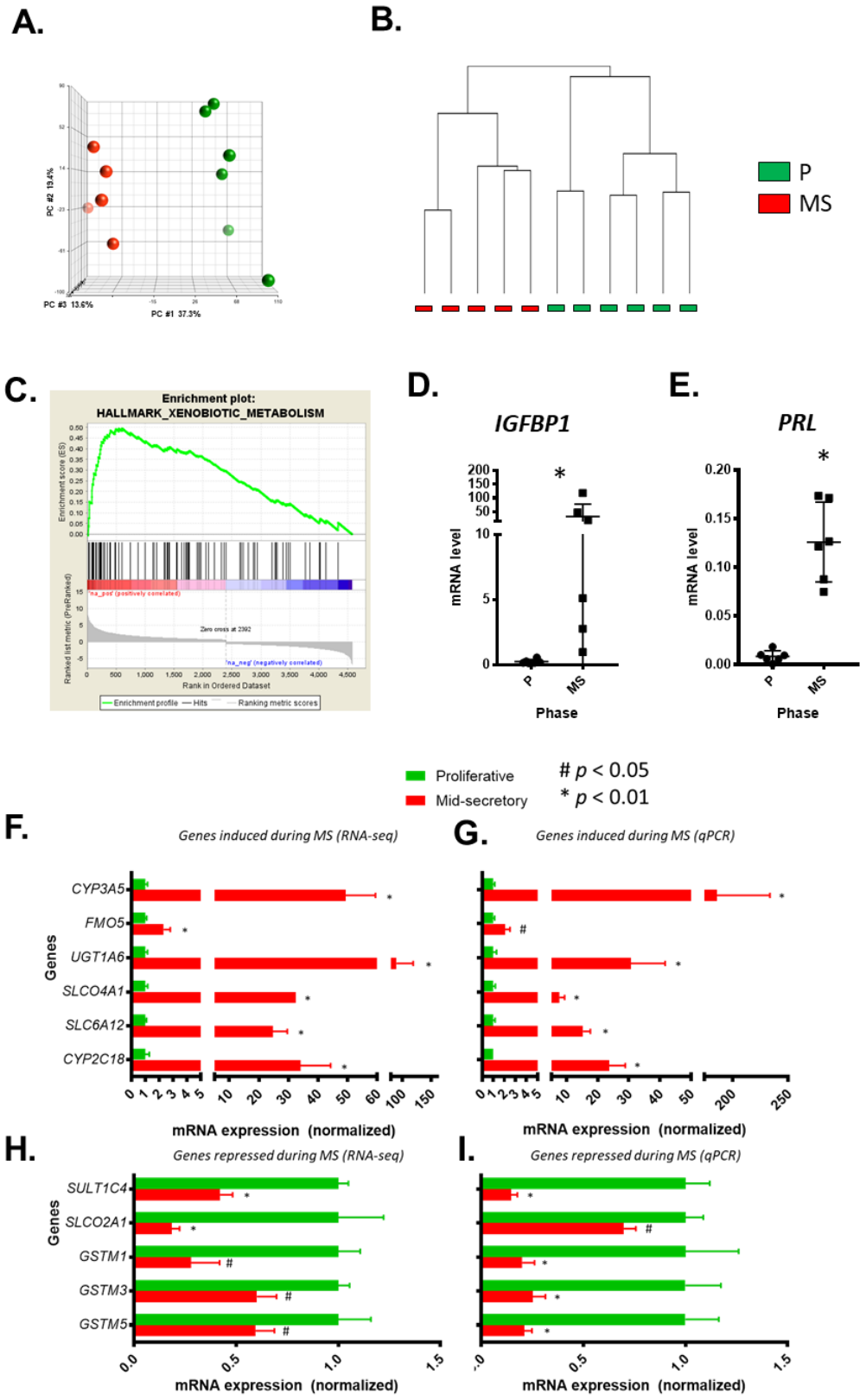
A.
PC #3 13.6%
PC #2 19.4%
PC #1 37.3%
B.
P
MS
C.
Enrichment plot:
HALLMARK_XENOBIOTIC_METABOLISM
Enrichment score (ES)
Ranked list metric (PreRanked)
Rank in Ordered Dataset
Enrichment profile
Hits
Ranking metric scores
D.
IGFBP1
mRNA level
Phase
E.
PRL
mRNA level
Phase
Proliferative
Mid-secretory
# p < 0.05
* p < 0.01
F.
Genes induced during MS (RNA-seq)
Genes
CYP3A5
FMO5
UGT1A6
SLCO4A1
SLC6A12
CYP2C18
mRNA expression (normalized)
G.
Genes induced during MS (qPCR)
mRNA expression (normalized)
H.
Genes repressed during MS (RNA-seq)
Genes
SULT1C4
SLCO2A1
GSTM1
GSTM3
GSTM5
mRNA expression (normalized)
I.
Genes repressed during MS (qPCR)
mRNA expression (normalized)

Figure 3.

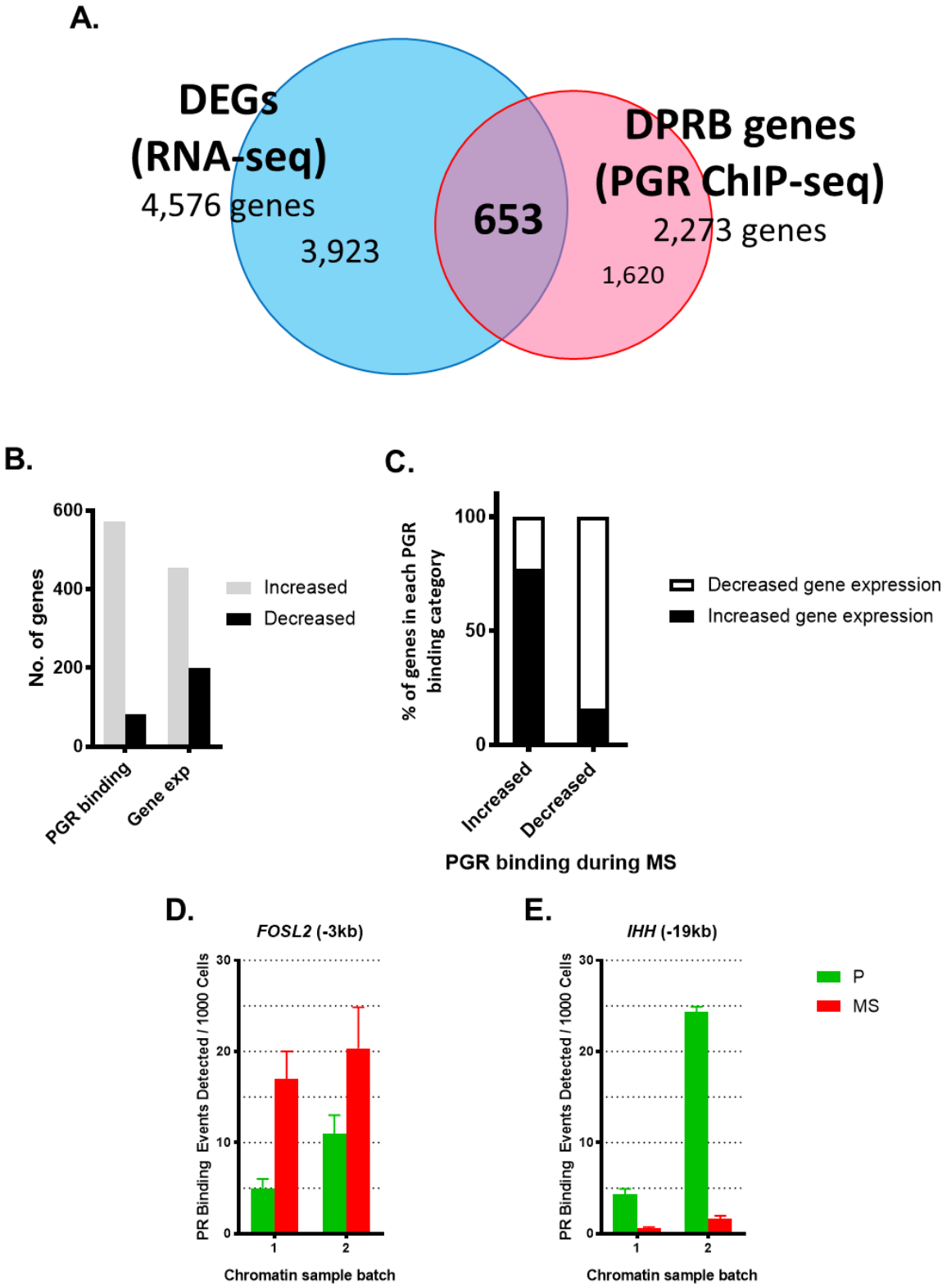
A.
DEGs
(RNA-seq)
4,576 genes
3,923
653
DPRB genes
(PGR ChIP-seq)
2,273 genes
1,620
B.
No. of genes
600
400
200
0
Increased
Decreased
PGR binding
Gene exp
C.
% of genes in each PGR binding category
100
50
0
Decreased gene expression
Increased gene expression
Increased
Decreased
PGR binding during MS
D.
FOSL2 (-3kb)
PR Binding Events Detected / 1000 Cells
30
20
10
0
1
2
Chromatin sample batch
E.
IHH (-19kb)
PR Binding Events Detected / 1000 Cells
30
20
10
0
1
2
Chromatin sample batch
P
MS

F.

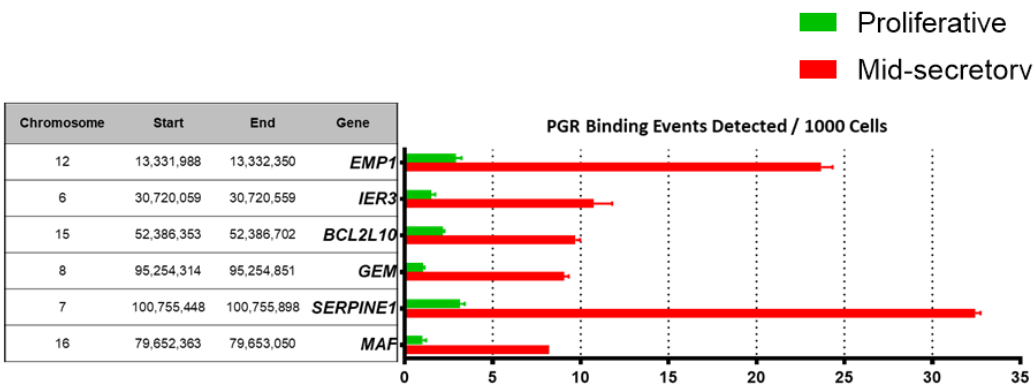

Chromosome	Start	End	Gene
12	13,331,988	13,332,350	*EMP1*
6	30,720,059	30,720,559	*IER3*
15	52,386,353	52,386,702	*BCL2L10*
8	95,254,314	95,254,851	*GEM*
7	100,755,448	100,755,898	*SERPINE1*
16	79,652,363	79,653,050	*MAF*

G.

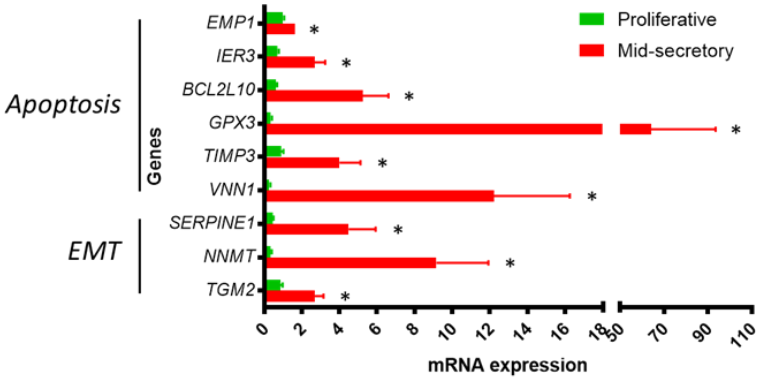

H.

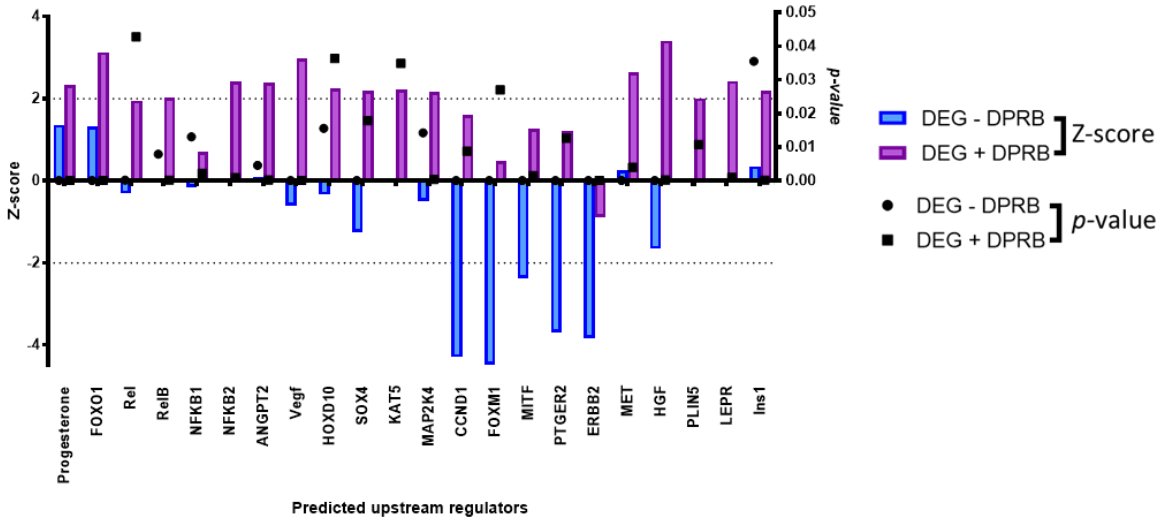

962

963

Figure 4.

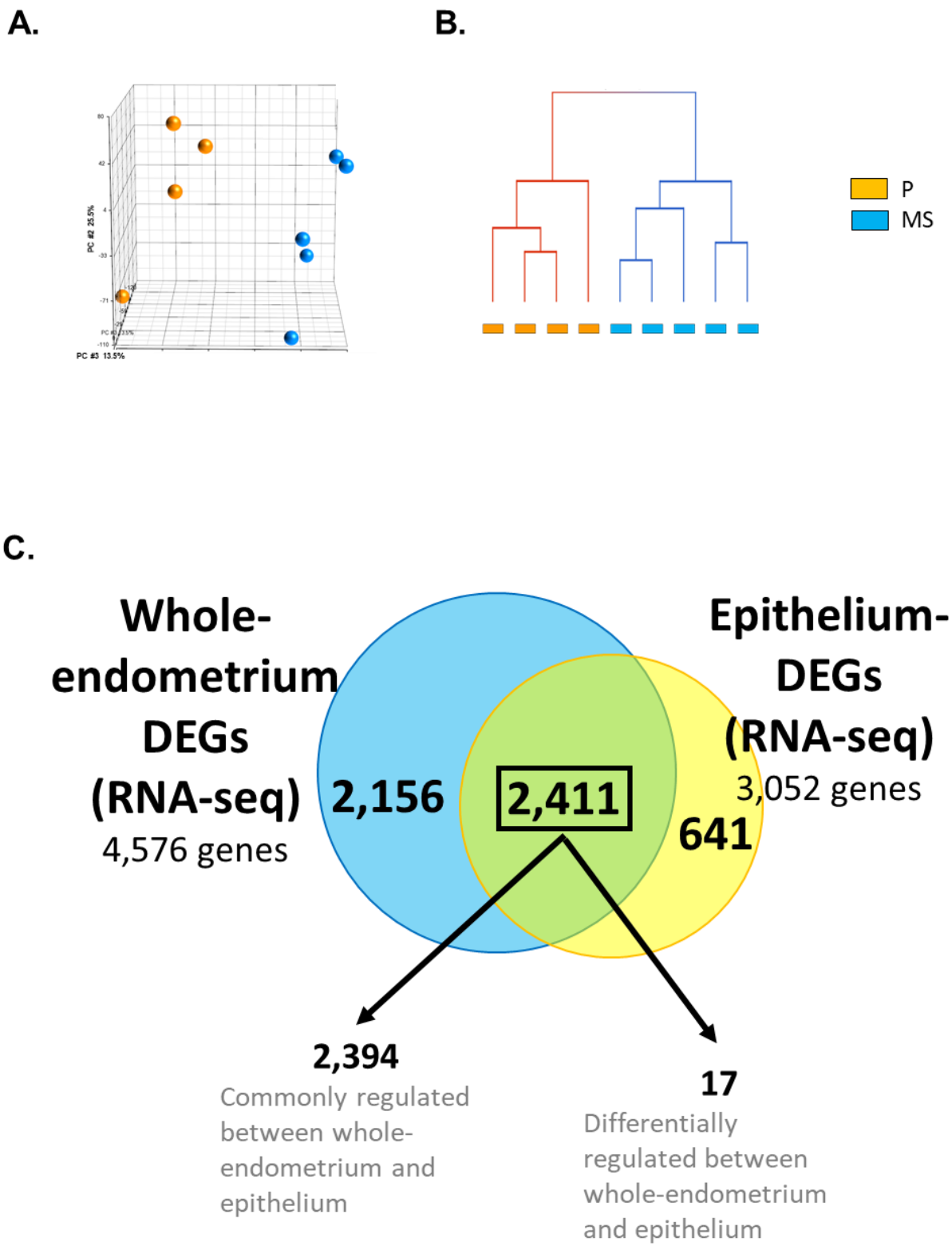
A.
B.
P
MS
C.
Whole-endometrium DEGs (RNA-seq)
4,576 genes
Epithelium-DEGs (RNA-seq)
3,052 genes
2,156
2,411
641
2,394
Commonly regulated between whole-endometrium and epithelium
17
Differentially regulated between whole-endometrium and epithelium

Figure 5.

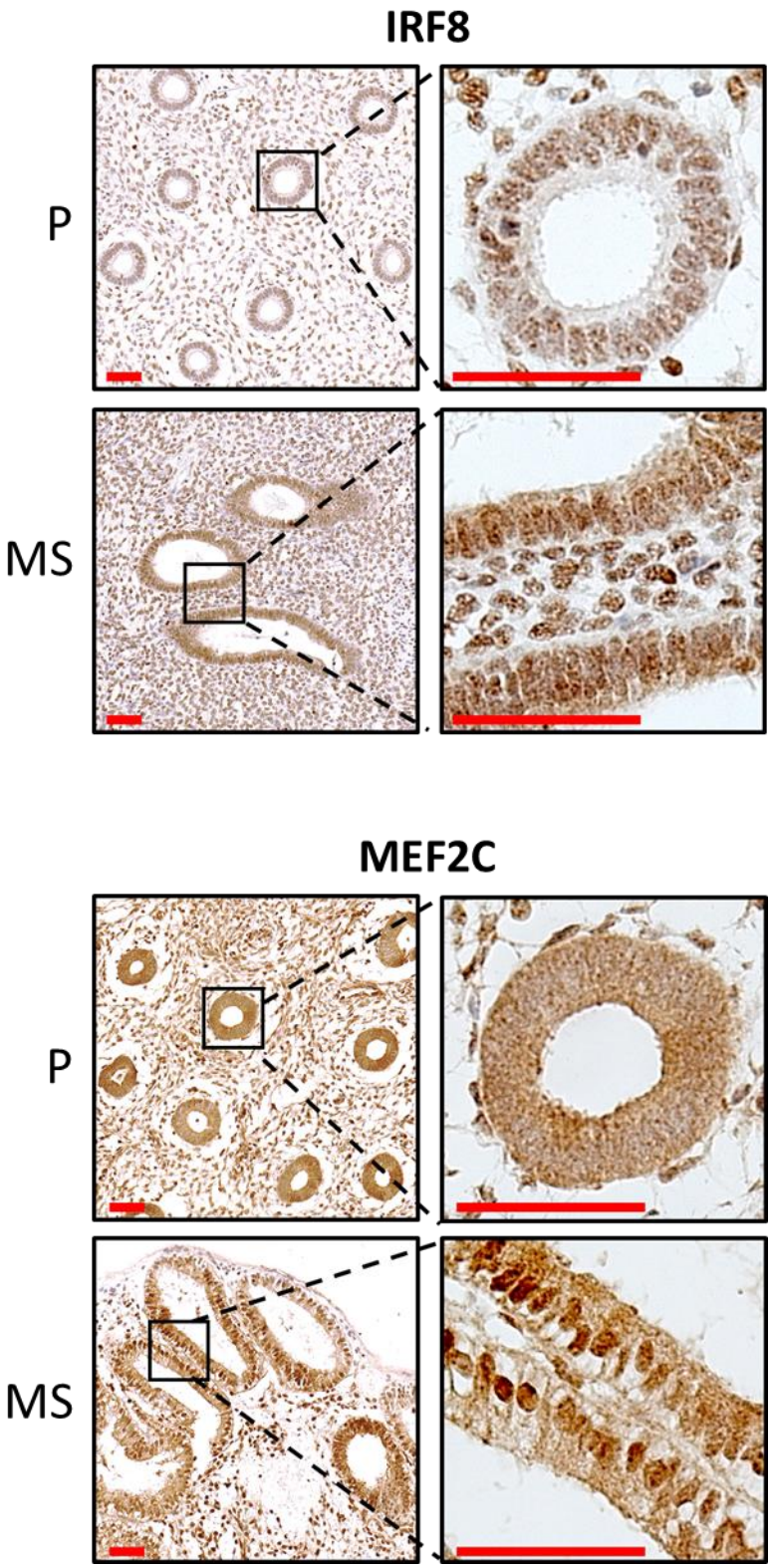

FIGURE LEGENDS

Figure 1. Genome wide PGR binding identified by ChIP-seq in endometrial tissue of fertile women during the proliferative and mid-secretory phases.

(A). Distribution of PGR binding in the genome relative to the gene body during the P and MS phase, as analyzed by PAVIS.

(B). Paired analysis was employed to identify differential PGR bound (DPRB) regions, where differential PGR binding was calculated for each batch consisting a P and MS pair. The DPRB DNA common to both batches were defined as the real differential PGR bound sites. A total of 2,787 PGR bound regions were found to be in proximity of 2,249 genes (TSS ± 25 kb).

(C). The percentage of total DPRB sites that showed increased (red) or decreased (green) PGR binding transitioning from P to MS.

(D). Gene Ontology functional annotation showing enriched biological functions associated with DPRB genes (defined as DPRB within 25 kb of transcriptional start sites), as analyzed by the online bioinformatic tool DAVID.

Figure 2. Endometrial gene expression profile during the proliferative and mid-secretory phases.

(A and B). Principal component analysis (PCA, A) and hierarchical clustering (B) using the gene expression profile for each individual sample derived from P (green) and MS (red) showed a clear segregation between the two phases.

(C). Gene Set Enrichment Analysis (GSEA) identified the xenobiotic metabolism pathway as significantly and positively enriched in the differentially expressed genes (DEGs), suggesting an increased activity in this pathway during MS.

(D and E). Decidualization markers *IGFBP1* and *PRL* were examined by qPCR using the independent patient samples to confirm stage of menstrual cycle.

(F - I). Selected genes from the xenobiotic metabolism pathway were validated by qPCR (G and I) using independent patient RNAs and presented in parallel with results from RNA-seq (F and H), n = 6, # $p < 0.05$ and * $p < 0.01$.

Figure 3. Identification of PGR regulated genes during the menstrual cycle.

(A). Overlaying the genes with DPRB and differential expression identified 653 such genes during the P to MS transition.

(B). Number of genes showing increased and decreased PGR binding and expression in the endometrium during MS.

(C). The percentage of genes showing increased or decreased expression with increased or decreased PGR binding from P to MS.

(D and E). PGR binding near two known target genes, *FOSL2* (D) and *IHH* (E) were examined by PGR ChIP-qPCR to confirm the phases of endometrial sample from which chromatin was obtained. qPCR was conducted in triplicates for each sample, results for both batch 1 and batch 2 are plotted.

(F). PGR occupancy was validated for selected genes from the xenobiotic metabolism, apoptosis and epithelial-mesenchymal transition (EMT) pathways using ChIP-qPCR. Experiments were performed using two different batches and a representative result is shown. * $p < 0.05$.

(G). Selected genes from the xenobiotic metabolism, apoptosis and EMT pathways were validated using qPCR, n = 6 and * $p < 0.05$.

(H). Comparison of the upstream regulator activity (as indicated by the Z-score) for DEGs with and without differential PGR binding. Activity status (Z-score) is plotted on the left Y-axis (blue and purple bars, representing without DPRB and with DPRB, respectively), and significance (*p* value) is plotted on the right Y-axis (circle and square, representing without DPRB and with DPRB, respectively).

Figure 4. Epithelial functions during implantation.

(A and B). Principal component analysis (PCA, A) and hierarchical clustering (B) using the gene expression profile for each individual sample derived from P (orange) and MS (blue) specifically in the epithelium, showing a clear segregation between the two phases.

(C). Comparison of DEGs derived from the epithelium to DEGs derived from the whole endometrium, with a total of 658 genes that were uniquely regulated in the epithelium.

Figure 5. Protein regulation of IRF8 and MEF2C in endometrial sections during P and MS.

Immunohistochemistry staining for IRF8 and MEF2C in human endometrial samples during P and MS. Results show that both proteins were expressed in both the epithelial and stromal compartment, but increased protein level and nuclear localization during the WOI was observed specifically in the epithelium for IRF8 and MEF2C, respectively. Experiment was conducted on three independent patients' samples and a representative is shown.

TABLES

TABLE 1. DAVID functional analysis using KEGG pathways for genes with differential PGR binding as determined by PGR ChIP-seq in the proliferative and mid-secretory endometrium

Term	P-Value	Genes
Insulin resistance	2.30E-04	*SREBF1, PIK3CG, IL6, IRS2, PTPRF, SOCS3, PRKAG2, NFKBIA, TRIB3, MAPK10, PPARGC1B, STAT3, PTPN11, SLC2A2, GFPT2, CREB3L2, CREB3L1, MLXIP, PTPN1, SLC27A3, PIK3R3, PIK3R2, PYGB*
Glycerophospholipid metabolism	2.70E-04	*CHKA, PLD1, PLB1, PISD, GPCPD1, LPIN2, LPIN1, CHPT1, LPCAT3, CDS2, GPD1L, PNPLA7, DGKD, PLA2G2A, DGKZ, LCLAT1, PLA2G2C, PLA2G2D, AGPAT3, PLA2G5, PLA2G2F*
Focal adhesion	1.70E-03	*PGF, BCAR1, PXN, CTNNB1, MYL9, COL6A6, ITGB8, PAK3, COMP, COL27A1, RAC1, PDGFC, PIK3R3, PIK3R2, PIK3CG, COL4A3, VAV3, TNXB, ACTN4, MYLK3, HGF, MAPK10, CAPN2, FLNB, COL5A1, VEGFD, LAMA3, ITGA6, RASGRF1, FYN, COL24A1, PARVB, PARVA*
Complement and coagulation cascades	3.20E-03	*PLAT, A2M, C3, C6, F13A1, C1R, BDKRB1, SERPING1, SERPINF2, SERPINE1, TFPI, SERPINA1, SERPIND1, CFD, PROS1*
Cytokine-cytokine receptor interaction	5.30E-03	*IL1R2, IL1R1, CXCR1, KITLG, CCL8, IL13, CXCR2, CXCR3, IL10, ACVR1B, CCL20, CXCR5, CXCR4, CLCF1, IL1RAP, CSF3R, PDGFC, CD27, IFNGR1, THPO, IL6, TNFSF4, HGF, TNFSF9, TNFSF8, IFNAR1, VEGFD, CCR7, TNFSF10, TNFSF11, CXCL14, PRLR, CCR2, IL22RA2*
Chemokine signaling pathway	9.50E-03	*ADCY7, BCAR1, CXCR1, CCL8, NFKBIA, CXCR2, FOXO3, CXCR3, PXN, CCL26, DOCK2, CCL20, CXCR5, CXCR4, RAC1, PIK3R3, PIK3R2, PIK3CG, VAV3, STAT1, STAT3, CCL17, CCR7, CXCL14, CCR2, IKBKG, GRK7, GRK5*
Ras signaling pathway	1.30E-02	*FGF14, PGF, KITLG, FGF12, RASAL2, PAK3, RAC1, TEK, PDGFC, RASA3, FGF1, PIK3R3, PIK3R2, PIK3CG, PLD1, HGF, MAPK10, RALGDS, PTPN11, VEGFD, PLCE1, RASGRF1, ETS1, ETS2, IKBKG, PLA2G2A, RIN1, PLA2G2C, KSR1, PLA2G2D, PLA2G5, PLA2G2F*

Proteoglycans in cancer	1.30E-02	*WNT5A, TFAP4, TLR4, MMP2, MIR21, TIMP3, PXN, CTNNB1, ANK1, CD44, RAC1, WNT6, PIK3R3, PIK3R2, PIK3CG, HSPG2, ESR1, HGF, FLNB, FZD7, ITPR1, STAT3, PTPN11, ITPR2, WNT2B, CTSL, SDC1, PLCE1, WNT9B*
FoxO signaling pathway	1.80E-02	*USP7, PIK3CG, IL6, IRS2, GABARAPL1, PRKAG2, SMAD3, BNIP3, MAPK10, FOXO3, IL10, STAT3, SOD2, TNFSF10, S1PR1, SETD7, FBXO32, PIK3R3, KLF2, GADD45A, PIK3R2*
Apoptosis	2.20E-02	*PIK3CG, CFLAR, TNFSF10, TNFRSF10B, CASP8, CASP12, IKBKG, NFKBIA, CAPN2, MAP3K14, PIK3R3, PIK3R2*
Prolactin signaling pathway	2.50E-02	*PIK3CG, TNFSF11, PRLR, SOCS3, SLC2A2, SOCS1, ESR1, MAPK10, FOXO3, STAT1, PIK3R3, STAT3, PIK3R2*
AMPK signaling pathway	2.60E-02	*SREBF1, PIK3CG, IRS2, PPP2R3A, PFKFB3, PPARG, PRKAG2, PFKP, FBP1, FOXO3, PPP2CB, CREB3L2, FASN, CREB3L1, PIK3R3, TBC1D1, PPP2R2C, LIPE, PIK3R2*
TNF signaling pathway	2.90E-02	*TRAF1, PIK3CG, CFLAR, IL6, SOCS3, NFKBIA, MAPK10, CCL20, CASP8, IKBKG, MAP3K8, CREB3L2, BCL3, CREB3L1, PIK3R3, MAP3K14, PIK3R2*
ECM-receptor interaction	9.40E-02	*COL4A3, TNXB, HSPG2, COL5A1, SDC1, LAMA3, ITGA6, COL6A6, CD44, ITGB8, COMP, COL27A1, COL24A1*

TABLE 2. Transcription factor binding sites enrichment in MS-gain intervals

Family	Transcription factor	p-value	Motif sequence
bZIP	FOSL2, FRA1, JUN-AP1, ATF3	1.00E-67	
bZIP	CEBP, CEBP:AP1	1.00E-64	
NR	GRE	1.00E-59	
bZIP	ATF4, CEBP:AP1	1.00E-52	
NR	AR	1.00E-41	
NR	PGR	1.00E-40	
bZIP	CHOP	1.00E-37	
STAT	STAT3	1.00E-34	
STAT	STAT1	1.00E-31	
STAT	STAT5	1.00E-30	

TABLE 3. Transcription factor binding sites enrichment in MS-loss intervals

Family	Transcription factor	p-value	Motif sequence
NR	ER	1.00E-20	
bHLH	TCF21	1.00E-11	
bHLH	ATOH1	1.00E-09	
ZF	ZBTB18	1.00E-09	
ZF	GLI3	1.00E-08	
bHLH	AP4	1.00E+07	
bHLH	NEUROD1	1.00E-06	
NR	AR	1.00E-05	
bHLH	TCF12	1.00E-05	
bHLH	ASCL1	1.00E-05	

TABLE 4. Gene sets enrichment analysis of the 4,576 DEG in whole endometrium

Enriched gene sets	Enrichment	NES*	NOM p-val	FDR q-val
TNFA SIGNALING VIA NFKB	Positive	2.37	0	0
XENOBIOTIC METABOLISM	Positive	2.24	0	6.48E-04
COAGULATION	Positive	2.19	0	4.32E-04
INFLAMMATORY RESPONSE	Positive	2.15	0	3.24E-04
COMPLEMENT	Positive	1.83	0.00159236	0.012257015
INTERFERON GAMMA RESPONSE	Positive	1.77	0.0015456	0.017625704
IL6 JAK STAT3 SIGNALING	Positive	1.70	0.00980392	0.031572554
APOPTOSIS	Positive	1.54	0.02276423	0.08806576
ANGIOGENESIS	Positive	1.46	0.0970696	0.122301854
E2F TARGETS	Negative	-3.12	0	0
G2M CHECKPOINT	Negative	-3.04	0	0
MITOTIC SPINDLE	Negative	-2.50	0	0
MYC TARGETS V1	Negative	-1.65	0.01590909	0.024345282
DNA REPAIR	Negative	-0.96	0.4974359	0.69968206

* NES = normalized enrichment score

TABLE 5. Genes with altered PGR binding and expression during P to MS transition

PR Binding	Gene expression	No. of genes (total = 653)	%
Increased	Increased	441	67.53
Increased	Decreased	131	20.06
Decreased	Increased	13	1.99
Decreased	Decreased	68	10.41

TABLE 6. Functional analysis of DPRB DEGs (categorized into upregulated and downregulated gene sets)

Enriched gene sets	Enrichment	NES	NOM p-val	FDR q-val
COAGULATION	Positive	1.85	0.001364257	0.0448207
INFLAMMATORY RESPONSE	Positive	1.59	0.037333332	0.2136788
TNFA SIGNALING VIA NFKB	Positive	1.59	0.026041666	0.1491825
XENOBIOTIC METABOLISM	Positive	1.57	0.03547963	0.1247853
EPITHELIAL MESENCHYMAL TRANSITION	Positive	1.55	0.038208168	0.1259948
COMPLEMENT	Positive	1.38	0.11479945	0.2892615
APOPTOSIS	Positive	1.37	0.092369474	0.2594335
HYPOXIA	Positive	1.31	0.1342711	0.3065951
INTERFERON GAMMA RESPONSE	Positive	1.29	0.17036012	0.302116
ESTROGEN RESPONSE LATE	Positive	1.15	0.31600547	0.4711447
IL2 STAT5 SIGNALING	Positive	1.13	0.31117022	0.4615895
P53 PATHWAY	Positive	1.12	0.32647464	0.4400889
MTORC1 SIGNALING	Positive	0.89	0.6025825	0.7500677
ESTROGEN RESPONSE EARLY	Positive	0.86	0.6555407	0.7511974
IL6 JAK STAT3 SIGNALING	Positive	0.76	0.7735584	0.8316847

TABLE 7. Gene sets enrichment analysis of the 3,052 DEGs in the epithelium

Enriched gene sets	Enrichment	NES	NOM p-val	FDR q-val
COAGULATION	Positive	2.4624	0.0000	0.00E+00
COMPLEMENT	Positive	2.3827	0.0000	0.00E+00
ALLOGRAFT REJECTION	Positive	2.3632	0.0000	3.45E-04
INFLAMMATORY RESPONSE	Positive	2.2584	0.0000	2.59E-04
TNFA SIGNALING VIA NFKB	Positive	2.1916	0.0000	6.29E-04
XENOBIOTIC METABOLISM	Positive	2.0994	0.0015	1.04E-03
HYPOXIA	Positive	1.9728	0.0014	5.53E-03
APOPTOSIS	Positive	1.8966	0.0015	1.17E-02
KRAS SIGNALING UP	Positive	1.8873	0.0000	1.17E-02
INTERFERON GAMMA RESPONSE	Positive	1.8572	0.0029	1.30E-02
IL6 JAK STAT3 SIGNALING	Positive	1.7955	0.0096	1.87E-02
EPITHELIAL MESENCHYMAL TRANSITION	Positive	1.7055	0.0058	3.26E-02
UV RESPONSE UP	Positive	1.6298	0.0210	5.45E-02
IL2 STAT5 SIGNALING	Positive	1.6076	0.0239	5.82E-02
ANGIOGENESIS	Positive	1.4423	0.0813	1.39E-01
APICAL JUNCTION	Positive	1.3225	0.1205	2.43E-01
P53 PATHWAY	Positive	1.2002	0.2147	3.96E-01
FATTY ACID METABOLISM	Positive	1.1766	0.2411	4.12E-01
MYOGENESIS	Positive	1.1574	0.2407	4.21E-01
E2F TARGETS	Negative	-3.7072	0.0000	0.00E+00
G2M CHECKPOINT	Negative	-3.4215	0.0000	0.00E+00
MYC TARGETS V1	Negative	-2.5766	0.0000	0.00E+00
MITOTIC SPINDLE	Negative	-2.5698	0.0000	0.00E+00
SPERMATOGENESIS	Negative	-2.3933	0.0000	3.69E-04
ESTROGEN RESPONSE LATE	Negative	-1.7289	0.0099	1.84E-02
PEROXISOME	Negative	-1.4721	0.0543	8.18E-02
OXIDATIVE PHOSPHORYLATION	Negative	-1.2415	0.1778	2.38E-01
DNA REPAIR	Negative	-1.1062	0.3187	3.82E-01
BILE ACID METABOLISM	Negative	-0.9779	0.4869	5.43E-01
MTORC1 SIGNALING	Negative	-0.7867	0.8145	7.83E-01

TABLE 8. Functional analysis of the epi-DEGs using IPA

Ingenuity Canonical Pathways	-log(p-value)	z-score	Molecules in dataset
Dermatan Sulfate Biosynthesis	3.67	-	*CHST1,HS6ST1,CSGALNACT2,SULT1A1,CHST10,HS6ST3,DSEL,SULT2B1*
Cholesterol Biosynthesis I	3.46	-	*FDFT1,EBP,MSMO1,CYP51A1*
Chondroitin Sulfate Biosynthesis (Late Stages)	3.41	-	*CHST1,HS6ST1,CSGALNACT2,SULT1A1,CHST10,HS6ST3,SULT2B1*
Superpathway of Cholesterol Biosynthesis	3.03	-	*FDFT1,EBP,MSMO1,HMGCS1,CYP51A1*
Chondroitin Sulfate Biosynthesis	3.01	-	*CHST1,HS6ST1,CSGALNACT2,SULT1A1,CHST10,HS6ST3,SULT2B1*
Osteoarthritis Pathway	2.18	2.496	*CXCL8,MTOR,FRZB,SMAD3,BMP2,ITGA2,BMPR2,WNT16,SOX9,MEF2C,HES1,ACAN,MMP1*
Cholecystokinin/Gastrin-mediated Signaling	2.15	2.121	*GAST,MAPK14,RHOB,MEF2D,CREM,MEF2C,GNA13,PRKCG*
IL-8 Signaling	2.03	2.309	*CXCL8,PIK3CA,MTOR,FLT1,RHOB,HBEGF,CXCL1,GNA13,KDR,MAP4K4,PRKCG,EIF4EBP1*
TGF-β Signaling	1.97	1.342	*IRF7,MAPK14,BMP2,SMAD3,BMPR2,TGIF1,INHBA*
PTEN Signaling	1.74	-2.121	*PIK3CA,FLT1,ITGA2,PREX2,BMPR2,KDR,BCL2L11,PDGFRB*

TABLE 9. Upstream regulators with specific actions in the epithelium

Upstream Regulator	Log2(FC) in epithelium	Molecule Type	Activation z-score	p-value of overlap
POU5F1	1.696	transcription regulator	2.429	3.93E-06
IRF5	1.526	transcription regulator	2.266	2.04E-04
MEF2C	1.098	transcription regulator	1.835	6.15E-03
MEF2D	1.014	transcription regulator	2.478	1.02E-03
IRF8	1.199	transcription regulator	1.608	3.35E-05
FOXJ1	-1.613	transcription regulator	-1.96	3.52E-02
TLR5	1.34	transmembrane receptor	3.062	7.08E-04
IL1R1	1.745	transmembrane receptor	2.872	2.27E-02
FCGR2A	2.025	transmembrane receptor	1.544	1.30E-04
MET	1.993	kinase	2.054	1.26E-09
AURKB	-3.136	kinase	-2.132	2.99E-03
HBEGF	1.739	growth factor	1.754	1.94E-05
WNT7A	-2.761	Wnt ligand	-1.98	2.60E-02
CYP27B1	-1.773	enzyme	-1.51	9.40E-03
DLL4	1.067	other	2.119	1.74E-05